

Technical Report: NAVTRADEVCEM 68-C-0152-1

AD 712793

A MATHEMATICAL MODEL FOR
ASSAULT BOAT MOTION IN WAVES

by

Paul Kaplan

Lawrence W. Ward

Theodore P. Sargent

OCEANICS, INC.
Technical Industrial Park
Plainview, New York 11803
Contract N61339-68-C-0152

JUNE 1969

D D C
RECEIVED
OCT 15 1970
REGISTERED
C

DOD Distribution Statement

This document has been approved
for public release and sale;
its distribution is unlimited.

NAVAL TRAINING DEVICE CENTER

ORLANDO, FLORIDA

INDC

ABSTRACT

A six degree of freedom mathematical model of an assault boat landing on and retracting off a sloping beach through surf is developed based on both theoretical and experimental results. Included are the effects of wave refraction, winds, shoaling, breaking and wave run-up on the beach. Control forces and moments resulting from the coxswain ability to alter the throttles and rudders are also included. This report is to serve as a basis for the development of a real time assault boat simulator for the training of coxswains.

ACCESSION for	
CFBTI	WHITE SECTION <input checked="" type="checkbox"/>
RDC	BUFF SECTION <input type="checkbox"/>
UNANNOUNCED	<input type="checkbox"/>
JUSTIFICATION	
BY	
DISTRIBUTION/AVAILABILITY CODES	
DIST.	AVAIL. AND SPECIAL
/	

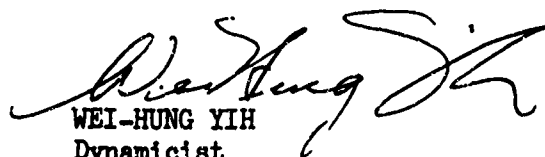
Reproduction of this publication in whole or in part is permitted for any purpose of the United States Government.

FOREWORD

The present study is to provide a mathematical representation of waves and surf typical of conditions encountered in the conduct of assault landings. The derived representations consist of equations giving the varying characteristics of a wave environment which affect the six degrees-of-freedom motion of an LCM(6) vehicle. These formulations, data and ideas will be useful in developing a real-time computer simulation of landing craft behavior in waves. The purpose of such a simulation relates to the Navy's need to produce alternate methods of training boat handlers. Development of the simulation at the Naval Training Device Center will involve verification and possible extension of the results documented here.



HARVEY C. SALTZMAN
Project Engineer
Naval Training Device Center



WEI-HUNG YIH
Dynamicist
Naval Training Device Center

TABLE OF CONTENTS

<u>Section</u>		<u>Page</u>
I	INTRODUCTION.....	1
II	STATEMENT OF THE PROBLEM.....	2
III	METHOD OF PROCEDURE.....	3
	<u>ANALYSIS</u>	3
	General.....	3
	Wave Characteristics in Shallow Water.....	4
	Breaker and Surf Characteristics.....	10
	Methods for Simulation of Wave Patterns.....	14
	Equations of Motion.....	17
	Hull Forces and Moments.....	21
	Propeller Forces.....	26
	Rudder Forces.....	29
	Control Forces.....	30
	Wave Exciting Forces and Moments.....	32
	Wind Effects.....	43
	Beach Forces.....	45
	<u>COMPUTATIONAL CONSIDERATIONS</u>	47
IV	CONCLUSIONS.....	51
V	REFERENCES.....	52
	APPENDIX A.....	65

LIST OF TABLES

<u>Table</u>		<u>Page</u>
1	Numerical Values of LCM (6) Ship Characteristics.....	55

LIST OF ILLUSTRATIONS

<u>Figure</u>	<u>Page</u>
1	Wave Propagation Toward Shore Along Sloping Beach.. 56
2	Variation of Wave Characteristics, Relative to Deep Water Values, as Function of Ratio of Depth to Deep Water Wavelength..... 57
3	Wave Refraction Diagram for Waves Approaching a Uniformly Sloping Beach, $\beta_0 = 45^\circ$ 58
4	Waves Approaching Beach Over Varying Bottom Contour, with Spatial Reference Point Locations..... 59
5	Sea State 4 Wave Spectrum Decomposition..... 60
6	Relation of Ship Axes, Shore Position, and Inertial Reference Frame..... 61
7	Variation of Propeller rpm with Speed at Self-Propulsion, Twin-Screws, Ahead Motion, Heavy Displacement..... 62
8	Variation of Propeller rpm with Speed at Self-Propulsion, Twin-Screws, Astern Motion, Light Displacement..... 63
9	Relation of Resultant Wind Velocity to Ship Axes... 64
A-1	Flow Diagram for Solution of Equations of Motion... 75
A-2	Flow Chart for Determining Oscillatory Wave Form and Forces..... 77
A-3	Flow Chart for Determining Solitary Wave Form and Forces..... 78
A-4	Procedure for Selecting Wave Forces..... 79

NOMENCLATURE

<u>Symbol</u>	<u>Description</u>
A'_{ii}	Component of added mass tensor ($i = 2$, along y-axis; $i = 3$, along z-axis)
A_{proj}	Projected abovewater area of craft, normal to resultant wind velocity
\bar{A}_z	Ratio of wave amplitude to heave amplitude for vertical motion-induced wave
a	Amplitude of surface wave evaluation at different locations along sloping beach
a_o	Deep water amplitude of surface wave elevation
B^*	Local beam of ship section
B	Ship beam
CB	Center of buoyancy
CG	Center of gravity
c	Propagation speed of surface wave
D	Propeller diameter
$D(\omega)$	Wave amplitude factor for effect of changing depth
d	Effective draft of equivalent rectangular block ship representation
$ GM $	Vertical distance between CG and meta- center
g	Acceleration due to gravity
H	Wave height
H_b	Wave height at breaking
h	Water depth along sloping beach
h_b	Water depth at breaking

<u>Symbol</u>	<u>Description</u>
h_0	Water depth at start of sloping beach
I_{xx}, I_{yy}, I_{zz}	Moment of inertia about x, y, or z-axis
$i = \sqrt{-1}$	Imaginary unit
$K(\omega, h)$	Wave amplitude factor due to refraction
K, M, N	Moment about x, y, or z-axis; also referred to as rolling, pitching or yawing moment
$k = \frac{2\pi}{\lambda}$	Wave number
$k_0 = \frac{\omega^2}{g}$	Wave number in deep water
L	Length along load waterline, used as reference length
a	Half-length of equivalent rectangular block ship representation
m	Mass
N'_{zx}	Local heave damping coefficient
n	Propeller rotational speed, rev./sec.
p	Pressure
p, q, r	Angular velocity component about x, y, or z-axis
R	Run-up magnitude
$S_n(\omega)$	Spectral energy of waves referred to a fixed position
T	Wave period, also used as symbol for propeller thrust
t	Time
U_W	Wind speed relative to inertial reference frame
U_{RW}	Resultant wind speed relative to the boat
u, v, w	Velocity components in the direction of x, y, or z-axis

<u>Symbol</u>	<u>Description</u>
u_0, v_0, w_0	Wave orbital velocity components in the direction of x, y, or z-axis
v_w	Wind speed used in definition of wave spectrum
$W = mg$	Weight
X, Y, Z	Component of force in the direction of the x, y, or z-axis; also referred to as longitudinal, lateral, or vertical force
x, y, z	Right-handed orthogonal system of moving axes, fixed in the body; the z-axis is directed toward the bottom of the body, with the x-z plane the vertical plane of symmetry of the body
x_b	Distance from initial offshore reference point to shoreline along x_0 -axis
x_0, y_0, z_0	Right-handed orthogonal system of fixed axes, referred to an inertial frame fixed relative to the earth surface with the z_0 -axis vertically down
x_{0b}	Location of wave breaking point along x_0 -axis
α	Beach slope
β	Wave refraction angle, relative to x_0 -axis (also used as sideslip angle of craft)
β_0	Wave angle relative to x_0 -axis, in deep water
$\gamma = \psi - \beta$	Angle between x-axis and normal to wave crests for unidirectional waves
δ	Angular deflection of rudder, positive for a clockwise rotation about z-axis (in radians)
ϵ	Parameter in solitary wave representation
η	Free surface elevation

<u>Symbol</u>	<u>Description</u>
θ	Pitch angle, about y-axis
λ	Wavelength
μ	Angle of resultant wind vector relative to the negative x-axis
ξ	Integration variable along x-axis
ρ	Mass density of water
ρ_a	Mass density of air
σ_η	Wave rms amplitude
ϕ	Roll angle, about x-axis
ψ	Yaw angle, about z_0 -axis
ω	Wave frequency, rad./sec.
ω_e	Encounter frequency, rad./sec.
ω_m	Wave frequency of maximum spectral density

Subscripts (Applicable to propeller operation)

o	Operating condition corresponding to twin screws operating in unison, or average of port and starboard propellers
p	Port side
s	Starboard side

SECTION I

INTRODUCTION

The development of adequate techniques for military personnel in carrying out their assigned tasks in connection with vehicle performance is often arrived at by the use of various training procedures. For one reason or another, it is often not possible or permissible to allow training to be carried out with the use of a vehicle, whether it be a ship, or aircraft, etc. In order to acquaint operational personnel with the elements they will experience in actual operation and/or control of such vehicles, recourse is made to the use of training devices. These devices provide a simulation of the realistic environment, obtained as a combination of visual displays and/or motion cues. In the case of training of an assault boat coxswain, there presently exists a limitation due to the unavailability of training boats; requirements of travel to training beach locations; and possible adverse weather and surf conditions. Thus a need arises for development of an assault boat coxswain trainer, where a mathematical model has to be derived for use in the training device computer in order to represent the vehicle motion and the wave conditions.

This project was carried out for the Naval Training Device Center under support of Contract No. N61339-68-C-0152.

SECTION II

STATEMENT OF THE PROBLEM

In the development of the trainer, it is necessary to represent the time history of the waves that are approaching a sloping beach, where the wave representation provides information on the wave system form in the vicinity of the assault boat as it approaches the beach. The equations for the waves will represent the wave properties and form up to surf formation when breakers are formed on the beach, and this wave system will continually affect the assault boat by providing wave-induced excitations that cause variations in the six degrees of freedom of a representative assault boat such as the LCM (6). In addition the vehicle motions will be affected as a result of the coxswain control, which is manifested by his ability to control the throttle, gear shift, and rudder, thereby determining the forward speed and the ship heading. The effects of wind are also included, since strong winds will create forces on the hull and will affect its motion in the horizontal plane, i.e. in the axial and lateral directions.

The present report presents the results of a combined theoretical and experimental study which has as its objective the development of a mathematical model that represents the six degrees of freedom motion of assault boats in waves. The model will also provide a time history of the waves along a sloping beach, in proximity to the assault boat, and it will allow treatment of the approach to the beach as well as the retraction operation of the boat returning from the shore to seaward. An important consideration in the mathematical model is the ability to obtain real time computer solutions, thereby permitting direct utilization in a training device with a man "in the loop" to provide control actions and observe their consequences. The mathematical model is presented in the present report, based upon many results obtained in an experimental model study in a towing tank [1]. The data analyses, approximations, computations, etc. providing further support for the proposed mathematical model, including verification and validation studies, are presented in an associated report [2] that represents the final descriptive report on this project.

SECTION III

METHOD OF PROCEDURE

A. ANALYSIS

1. GENERAL

The techniques used in deriving the equations presented herein represent the application of the present state of the art in accounting for motions of ships in waves. As such linear theory is primarily used, with appropriate expansion to encompass certain nonlinear effects when they are considered to be significant. A similar treatment is applied when considering the waves as they progress into shore and affect the boat motion. However since the major objective of this study is to obtain a mathematical model that will suffice for application in a training device, certain approximations are made in order to allow simplification and achieve results useful for that purpose. Thus the precision associated with a detailed research program directed toward shallow water wave effects on ships; complete details of wave form for breakers; determination of the change in all of the spectral properties of waves along a sloping beach; etc. is not achieved in this work, but nevertheless a utilitarian tool adequate for training purposes is obtained. The foregoing represents the fundamental philosophy underlying the development of the mathematical model described in this report.

In formulating the equations of motion all six degrees of freedom of the boat are represented. In the usual case of a ship in waves, the vertical plane motions of pitch and heave are formulated according to linear theory (see [3] and [4]) for a fixed forward speed, and the effect of surge is neglected. However in the present case where forward speed control is manifested by the coxswain controlling the engine, and also using the ability to apply differential thrust as a means of controlling heading, the surge degree of freedom (i.e. axial motion) is coupled with the lateral plane motions as well as the vertical plane motions. The nature of the coupling is both linear and nonlinear, and the functional form resulting will be the most simple possible in order to achieve the required ease of computer representation and solution.

The wave motion is represented in a time history form for regions in proximity to the boat, thereby allowing incorporation into a proposed training device since the view of the local wave environment is then available in conjunction with a simulated boat motion. The wave representation includes the effects of shoaling, which represents the influence of the sloping beach depth changes on the wave properties, as well as refraction effects that account for the influence of changing depth on the direction of wave propagation as the shoreline is approached. Methods allowing evaluation of deterministic properties of waves of sinusoidal form (initially, in deep water) as they

progress onto the beach, as well as for a prescribed spectral distribution of irregular random waves, are included.

The equations of motion for the boat in regular waves are formulated on the basis of linear theory initially, by the balance of inertial, damping, restoring, coupling, and wave excitation forces and moments. Both hydrodynamic and hydrostatic effects of body-fluid interaction are included, with many terms determined by application of the technique denoted as strip theory (a form of slender-body theory), as demonstrated in [3] and [4]. This method makes the assumption that, for an elongated body with transverse dimensions small compared to its length, the flow at any cross-section is independent of the flow at any other section, and hence the flow problem is reduced to a two-dimensional problem in the transverse plane. The forces at each section are found by this method, and the total force is found by integrating over the body length. While this theoretical technique has been found useful for heave and pitch motions in waves for a ship at a fixed forward speed, the presence of the other modes of motion together with the influence of forward speed control requires obtaining extensive model test data for the various hydrodynamic forces that act on a landing craft. Accordingly a model test program was carried out for this purpose, and the results presented in [1]. The data from that report, when analyzed and reduced to the required final form, yielded much of the information required for application to the present mathematical model, and a description of the techniques used to obtain the necessary hydrodynamic information is presented in [2], the complete final report for this project.

The particular assault boat studied in detail in this program is the LCM (6). Information on the operation of this craft, as well as some description of its physical characteristics, is provided in [5]. Body lines, section characteristics, rudder profile, propeller outlines, etc. were obtained from [6]. This particular craft has twin screws, both of which are right-handed and offset from the ship centerline. Twin rudders are also present, protected by skegs, and lying aft of the propellers. The rudders operate in unison, and they are controlled by one wheel in the pilothouse. Two displacements are considered, the heavier one being the condition when the craft approaches the beach fully loaded and the lighter being the condition for the craft leaving the beach empty. A summary of the numerical values of the important parameters characterizing the LCM (6), for which the present mathematical model was derived, is presented in Table 1.

2. WAVE CHARACTERISTICS IN SHALLOW WATER

In order to illustrate the basic characteristics of waves as they propagate toward a beach from deep water, the fundamental equations for amplitude, wavelength, and direction changes are presented in the following. Initially there are considered to be plane waves offshore of frequency ω (rad./sec.),

amplitude a_0 , and wave direction angle β_0 , and they are travelling shoreward over a prismatic bottom towards a parallel shoreline, as shown in Figure 1. With the assumption of conservation of energy and frequency and no reflection of the waves, as in the case of a slowly varying bottom contour of known depth $h(x)$, the inshore wavelength λ , amplitude a and wave direction angle β can be predicted; however no attempt is made in the analysis to determine the phase of the waves. Assuming small amplitude and using the principle of linear superposition this can also be extended to an offshore spectrum of waves with amplitudes distributed according to frequency.

For the case of a simple plane wave of frequency ω travelling in a direction perpendicular to the beach, hydrodynamic wave theory [7] yields the result

$$a = a_0 D(\omega) \quad (1)$$

where

$$D = \left[\frac{\frac{k}{k_0}}{1 + \frac{2kh}{\sinh 2kh}} \right]^{1/2} \quad (2)$$

and

$$k_0 = \frac{\omega^2}{g} = k \tanh kh \quad (3)$$

A graph of the relationship in Equation (3) is shown in Figure 2, together with other relations covering wavelength, slope, etc. In all cases inshore $k > k_0$ is valid, so that the corresponding wavelengths $\lambda = \frac{2\pi}{k}$ are therefore less than those offshore. The wave amplitudes are found to first decrease in moderately deep water and then increase in very shallow water, but in all cases the wave steepness increases in shallow water. All of the results obtained in the foregoing analysis are general, and not restricted to any particular bottom contour.

In the case of waves approaching the beach at an offshore angle to the beach β_0 , refraction takes place. For a beach whose depth decreases monotonically with x inshore, the wave angles decrease and the crests tend to be parallel to the beach far inshore. The controlling relationship, referred to as "Snells Law" [7] is

$$\sin \beta = \frac{k_0}{k} \sin \beta_0 \quad (4)$$

There are corresponding amplitude variations due to converging of the wave rays, so that in the case of refraction

$$a = a_0 KD \quad (5)$$

where

$$K = \left[\frac{\cos \beta_0}{\cos \beta} \right]^{1/2} \quad (6)$$

and D is as given previously in Equation (2). An illustration of the refraction of waves is given in Figure 3, for the case where $\beta_0 = 45^\circ$ and the beach is straight with parallel depth contours. The trend toward crests parallel with the beach will maintain itself until breaking occurs, which will determine the actual direction of the waves relative to the beach at the shoreline.

The wave system characteristics described above are based on linear theory, and hence have a restricted validity as the wave progresses into more shallow water and approaches the shoreline. The wave shape will begin to change from the sinusoidal form and the effects of breaking then manifest themselves, with the phenomenon then being nonlinear and complex. A discussion of these effects will be given in a later section, while the present discussion is sufficient to provide a general description of the major overall properties of the waves.

A deterministic approach, similar to that in [8] and [9], can be applied to the case of waves travelling into shallow water from an offshore deep depth location. In order to simplify the analysis the waves offshore are assumed at first to be travelling perpendicular to the beach, and the waves are measured with respect to an absolute frame of reference rather than with respect to the moving craft.

Consider waves as shown in Figure 4 moving from offshore to inshore in the direction of x over a bottom of slowly varying depth $h(x)$, with the latter variation slow enough to insure complete transmission of energy without reflection. This results in the connection between the amplitude a of the waves and the offshore amplitude a_0 , discussed previously and defined by Equations (1)-(3).

A precise presentation of the waves at a particular point, with reference to their form (as a function of time) at another point, can be achieved in a simple manner, where any change in phase is indicated directly. This can be done for a single sinusoidal wave form and generalized to an arbitrary wave system, following the techniques in [8], [9]. The same type of result can also be obtained for the case where the waves travel to some angle other than normal to the beach, which would include the effect of refraction as well. However a detailed consideration of this particular technique was found to be difficult to implement for the present problem due to the requirement of accounting for the influence of the craft forward speed (which varies with time); anomalies associated with

relations between wave frequencies and frequency of encounter in following seas; and expected computational requirements that inhibit real-time simulation of the wave system in this case. This approach would only have use for determining the exact representation of a simplified wave system, or for a spectral distribution of irregular waves, if the instantaneous phase were required. Since the application of the results in this study are for simulation purposes, only conditions representative of what occurs are required. Actual wave systems at sea are irregular random processes [10], and they are represented as a summation of many individual waves of various frequencies, each with a random phase, so that the necessity for representing phase relationships precisely is not present for this investigation. Thus a simplified treatment for representing component waves that make up an actual wave spectrum is used, thereby allowing ease of computation as well as a simple means of representing the wave forces associated with such wave systems.

To illustrate the above, consider a single component plane wave of frequency ω and amplitude a_0 offshore propagating inshore towards a beach located at $x = x_b$. The special case of a constant slope linear beach defined by

$$h = h_0 - \alpha x \quad (7)$$

with

$$\alpha = \frac{h_0}{x_b} \quad (8)$$

is the prescribed depth variation considered throughout this study, for simplicity. The offshore wave is represented by

$$\eta = a_0 \sin(kx - \omega t) \quad (9)$$

and at the point x_1 the wave is given by

$$\eta = a_1 \sin(k_1 x_1 - \omega t) \quad (10)$$

where

$$a_1 = a_0 D_1 \quad (11)$$

with the values of D_1 and k_1 found from Equations (2) and (3), using the local depth value

$$h_1 = h_0 - \alpha x_1 \quad (12)$$

Similarly at the point x_2 ,

$$\eta = a_2 \sin(k_2 x_2 - \omega t) \quad (13)$$

with similar relations for a_2 , k_2 , and D_2 in terms of the local

depth h_2 , etc.

In order to represent the effect of refraction on the preceding results, a single component plane wave of frequency ω at an initial angle β_0 offshore is considered progressing inshore. Assuming no reflection from the beach, the wave continuously refracts at the angle β until it finally arrives at the beach, where the relationship between β and β_0 is given by Snell's law, Equation (4). The amplitude of a plane wave travelling inshore at an angle β to the x-axis is

$$\begin{aligned} \eta &= a \sin \left[k(x \cos \beta + y \sin \beta) - \omega t \right] \\ &= a \sin \left[k_x x + k_y y - \omega t \right] \end{aligned} \quad (14)$$

where

$$\begin{aligned} k_x &= k \cos \beta \\ k_y &= k \sin \beta = k_0 \sin \beta_0 = \text{constant} \end{aligned} \quad (15)$$

(according to Snell's law).

Refraction and shoaling affect the wave amplitude according to

$$a_i = K_i D_i a_0 \quad (16)$$

where K_i and D_i are defined in Equations (2) and (6), and the i -subscript relates the spatial locations considered. The latter relation assumes no reflection of energy while proceeding into the beach and total absorption of energy at the beach, as noted previously. The relations above provide the means to predict the detailed behavior of waves at different inshore points given the beach slope and the frequency, amplitude and direction of the waves at an offshore point. Thus,

$$\eta_1 = a_1 \cos \left[k_{x_1} x_1 + k_{y_1} y_1 - \omega t \right] \quad (17)$$

at point (x_1, y_1) , and

$$\eta_2 = a_2 \cos \left[k_{x_2} x_2 + k_{y_2} y_2 - \omega t \right] \quad (18)$$

at (x_2, y_2) , in accordance with the method described above, where

$$\frac{a_2}{a_1} = \frac{K_2 D_2}{K_1 D_1} \quad (19)$$

and the K_i -values are found in terms of the local depth h_i .

The preceding discussion considered the characteristics of the waves when viewed from an absolute frame of reference, but the present problem requires consideration of the wave characteristics, time history, etc. in proximity to the assault boat while it is moving at some forward speed. When the boat approaches a shoreline, the seas are generally in the same direction as the craft forward motion, and hence are following and overtaking seas. When the craft is retracting from a beach and going seaward it will be proceeding opposite to the wave propagation direction, and hence the seas will be head seas relative to the boat. The main effect of the forward speed of the boat is to alter the frequency of encounter of the waves relative to the boat, with different influence and consequences in each case. Assuming pure head sea operation, the frequency of encounter in deep water is given by

$$\omega_e = \omega + \frac{\omega^2}{g} u \quad , \quad (20)$$

assuming constant forward speed u . For the situation where the boat approaches the beach, with the waves as pure following seas, the frequency of encounter (assuming deep water and constant speed) is represented by

$$\omega_e = \omega - \frac{\omega^2 u}{g} \quad (21)$$

The change in the frequency of encounter due to forward speed in shallow water, just as in the case of deep water, is exhibited by the following relations:

$$\omega_e = \omega + ku \quad (22)$$

for head seas, and

$$\omega_e = \omega - ku \quad (23)$$

for following seas. Since the wave number k varies with position along the beach in the shallow water case, the frequency of encounter will vary as the boat moves along the sloping beach. However, a knowledge of the ship speed and its position along the beach (thereby providing information on the local depth) will allow computation of the change in frequency of encounter.

The effect of forward speed also manifests itself in a reshaping of the wave spectrum as a function of ω_e (see [10]).

This effect is important if a continuous change in the wave spectrum is to be applied as a function of craft position and time, which would be an impractical technique for simulation purposes. Consideration of this encounter spectrum only provides insight into the particular wavelengths that would have significant influence on ship motions, but that is only important for purposes of analysis rather than application to simulation, which is the prime purpose of this study.

Since the forward speed of the craft will generally vary due to wave effects and coxswain control inputs, the use of a frequency of encounter is only limited to interpretive purposes and simplified illustrations. When considering wave representations, wave-induced forces, etc. relative to the moving craft the "argument" of the defining sinusoidal functions will be

$$\left(\omega t \pm k \int u dt \right) \quad (24)$$

and discussion of the applicability of this term will be provided in a later section.

3. BREAKER AND SURF CHARACTERISTICS

As indicated previously, the wave height of a wave approaching a shoreline will increase as it progresses closer to the shore, and eventually reaches a condition where the wave form changes and the wave then becomes unstable and breaks. The breaking is characterized by the formation of turbulence as water spills from the crest while the wave advances, and also by means of the entire crest falling forward in a plunging form and dissipating its energy in the turbulence associated with the breaking process. The surf zone is a region where the waves tend to be quite steep, and it extends from the outermost breakers to the region where the water is rushing up the beach. In this region nonlinear processes become very important, and consequently it is the region which is least amenable to theoretical treatment. Many observations of breaker characteristics have been made experimentally, and the nature of the breakers is defined in accordance with the manner of breaking, as a function of the original deep water wave slope and the beach slope (see [11]).

When regular waves propagate inshore, they retain their sinusoidal outline until the ratio of the depth to deep water wavelength reaches the condition

$$\frac{h}{\lambda_0} = .04 + 1.35 \frac{H_0}{\lambda_0} \quad , \quad \text{for } \frac{H_0}{\lambda_0} \geq .01 \quad (25)$$

where H_0 and λ_0 are the deep water height and wavelength. This relation is based upon results presented in [11], where the minimum depth to which wave height theories apply for wave transformations in shoaling water is illustrated. After that point considerable departure from the theoretical outline occurs, with such departures dependent on the original wave steepness. The hydrodynamic theory of waves of finite height [7] indicates that breaking occurs when the crest angle is 120° , with the particle speed at the crest equal to the wave speed c , and the particle acceleration equal to that of gravity. The maximum steepness for such a wave in deep water is found to be

$\frac{H}{\lambda} = 0.142 \approx \frac{1}{7}$, with an actual indication of the phase speed about 10% greater than that from linear theory. Since the breaking of waves is a nonlinear feature, only limited information for mathematical models can be obtained from a linear analysis, and an approximation is necessary in the present study.

The wave representation in the present investigation will not allow "foaming", "white horses", etc. that dissipate wave energy by partial breaking at the top of the crest. This is usually associated with steep waves in deeper water as they run into shallow water, and they break so that the maximum steepness is maintained at a certain level. The breaking characteristics for such waves are quite different from those for low long waves offshore, which are a more appropriate condition for the present case. For those waves the wave profile inshore tends to concentrate the wave energy into the crest, where the crest rises and occupies only a small fraction of the total wavelength, with the trough becoming relatively flat and occupying the major portion of the wavelength. Thus the final pattern is a series of isolated steep crests separated from each other by long flat troughs which appear to have only a little depression below the mean water level. Such waves then break at relatively large heights producing a significant "run-up" along the beach.

An approximation to the wave characteristics in shallow water just prior to breaking can be obtained by use of the solitary wave concept. While the agreement is not precise for certain aspects of the wave characteristics, the approximation of the solitary wave is a sufficiently good representation that allows a useful mathematical form for the waves. This form is also applicable to the determination of the excitation forces associated with such a wave acting on a boat as it approaches the beach. Thus a mathematical model of the solitary wave is used for such purposes in this study.

Since the breaker height and the depth at which breaking occurs depend upon the beach slope and the deep water wave slope, a single relationship that is unique for all conditions is difficult to find. However, as an approximation, the limiting condition for solitary wave height relative to the depth is used as a representation of an effective criterion for establishment of the breaker conditions. This result is represented by the relation

$$\frac{H_b}{h_b} = \frac{5}{7} \approx .714 \quad (26)$$

where the b-subscript corresponds to breaking conditions, which will be used as an approximation in the present work. The procedure to be used in the mathematical model is to determine the local (maximum) wave height at the location corresponding to the condition given in Equation (25), and then to assume

that the solitary wave has the height corresponding to that magnitude at that point. The solitary wave then propagates along the sloping beach in accordance with the basic relations defining such a wave. A series of solitary waves can repeat themselves at the same period as a single oncoming sinusoidal-form wave assumed present in deep water offshore (the original wave), but in the case of a spectral distribution of waves offshore an approximation can be made to use the period of maximum spectral energy of the particular deep water spectral distribution.

The height of each particular solitary wave will vary with the local depth in the same manner as an ordinary small amplitude wave, i.e. according to the classical Green's law for shoaling waves, i.e.

$$\frac{H_2}{H_1} = \left(\frac{h_1}{h_2} \right)^{1/4} \quad (27)$$

which relates the heights at two points in terms of their local depths. The solitary wave form propagates in this manner until the limit condition given by Equation (26) is achieved, at which time breaking can be said to occur. The basis for using the solitary wave is the similar appearance of solitary waves to breakers (i.e. spilling breakers) and the tendency to form a relatively high pulse-like wave elevation. The approach is that of a quasi-steady variation, where at each instant a steady state representation of the solitary wave is used in accordance with the variations caused by local depth changes along the sloping beach. A practical reason for use of this model is the complicated requirement of applying numerical techniques such as the method of characteristics (e.g. [12]) or the Lagrangian method of [13] to continuously compute the wave form as an actual unsteady problem up to the point of breaking. The actual breaking conditions are not properly represented by either of the latter approaches, and their computational complexity limits their utility. This is especially significant since it is necessary to use the hydrodynamic wave system to determine the wave-induced forces on a craft in a real-time computation where representation of the waves in both space and time is required.

The equation representing the wave form for the solitary wave, assuming that it is propagating along the positive x_0 - direction, is given by [11] as

$$\eta = H \operatorname{sech}^2 \left[\sqrt{\frac{3H}{4h^3}} (x_0 - ct) \right] \quad (28)$$

where

$$c = \sqrt{gh} \left(1 + \frac{1}{2} \frac{H}{h} \right) \approx \sqrt{g(h+H)} \quad (29)$$

is the wave propagation speed, and H is the height of the wave

above the still-water level corresponding to the local depth h . The expression in Equation (28) provides a representation of the variation of the wave form as a function of space and time, where the height changes in accordance with the relation given in Equation (27) as the wave progresses along the beach. This expression is valid for the case of the wave propagating in a direction normal to the shoreline, as observed in a fixed frame of reference.

Since use of the solitary wave representation as an equivalent to the breaker form occurs in relatively shallow depths, it is assumed that no further refraction occurs and that the wave propagates at the angle appropriate to the condition where "transition" occurs between the sinusoidal wave forms and the solitary wave. The representation of the wave, at the angle corresponding to the transition orientation (denoted as β_t), is given by

$$\eta_m = H \operatorname{sech}^2 \left[\sqrt{\frac{3H}{4h^3}} \left\{ x_0 \cos \beta_t + y_0 \sin \beta_t - ct \right\} \right] \quad (30)$$

This wave orientation will maintain itself up to breaking, beyond which no further wave form is considered to exist.

Following the occurrence of breaking, a form of "wave of translation" or bore is assumed to exist in the water, and this produces a certain run-up on the beach, where the run-up is the vertical distance between the maximum height the water runs up the beach and the still-water level. The magnitude of the run-up is given by [14], as obtained from a large series of experiments. It is given as a function of the deep water wave height and period, and for the present investigation the deep water wave height reference is selected as the significant height offshore, where the significant height is the mean of the one-third highest waves, which is given by

$$H_0 \text{ sig.} = 4\sigma_{\eta_0} \quad (31)$$

with σ_{η_0} the rms wave amplitude in deep water. The reference period for the evaluation of the run-up is the period of maximum spectral energy, $T = \frac{2\pi}{\omega_m}$. In the evaluation of the conditions for the transition to a solitary wave, expressed by Equation (25), the deep water wavelength chosen for that case is the value associated with the deep water wave frequency ω_m , consistent with the assumptions used in this treatment.

It is very difficult to predict the magnitude of the velocities in the water advancing up the beach following breaking, since that is dependent on the value of the beach slope, friction

effects on the bottom, fluid mixing processes, etc. However, it is possible to approximate the value of the longitudinal velocities in the fluid after breaking by applying some of the results of [15], with the assumption that the water region after breaking is represented by a constant increased height about the undisturbed water level equal to the run-up R . Thus a uniform height of fluid is assumed to exist from the end of the breaking wave up to the shoreline, where the instantaneous height of water above the "ground" level of the beach is $(h+R)$, where h is the local depth below the undisturbed water level. Assuming that the propagation speed of this bore is

$$c_R = \sqrt{g(h+R)} \quad (32)$$

similar to the relation for the solitary wave given in Equation (29), the results in [15] indicate that the longitudinal particle velocities in this bore are represented by

$$u_R \approx .5 c_R \quad (33)$$

This rush of water toward shore is assumed to occur after breaking, and exists for a period of about $\frac{T}{2}$, where $T = \frac{2\pi}{\omega_m}$, and this repeats itself after each breaking wave.

From the point of view of action on a boat, when it is landing, stationary on the beach, or retracting (as long as it is located in the region between the breaking wave and the shoreline), the effect of this fluid motion is also to elevate the fluid level by the magnitude of run-up R above the still water level. This change occurs as a time-varying form which can be represented initially as a rectangular pulse with some sort of decay so that the return to level water conditions is present. Since it is difficult to deal precisely with the seaward return and backwash of the water mass following breaking, this method of approximation is considered sufficient. Techniques for carrying out the necessary computations (with a digital computer) that represent the various aspects of the waves, viz. oscillatory wave systems, solitary waves, and the bore characteristics following breaking, are discussed in the following section of the report.

4. METHODS FOR SIMULATION OF WAVE PATTERNS

In order to represent the waves at various points inshore as the boat progresses, it is necessary to determine them from the initial deep water waves that exist further out at sea. For the present case the waves must be determined as functions of time and spatial location, whether observed at a fixed point or when located on a moving craft. A simulation tool that has been used extensively in representing waves, when considering a random sea, is to obtain a time history record from the output of a white noise generator that is sent

through a spectrum-shaping filter. The amplitude characteristics of this filter are proportional to the square root of the desired wave power spectral density at each frequency in the wave bandwidth, and the output signal is then a single realization of a time series record having the desired power spectrum. This record serves as the deep water wave system, and appropriate operation upon it can produce the inshore waves and records of other wave-related quantities via convolution methods [8] (when that method is applicable) or by varying the spectrum in terms of local depth. An alternate method can be applied to a given offshore wave spectrum, where the spectrum is divided into a number of strips of different bandwidths and each strip is represented by a sinusoid whose magnitude and frequency are given by the square root of the area of the strip and by the median frequency of the strip. This representation produces a wave output record that appears random and is a sufficient basis for representation of the particular wave spectrum of interest. When the spectrum is divided into a finite number of sinusoids, it is relatively easy to determine the resultant inshore waves, wave forces, and other quantities used in a simulation study. The number of waves chosen to represent a given offshore spectrum, and an illustration for the particular case of Sea State 4, using 8 component waves, is shown in Figure 5.

Each of the constituent sinusoidal functions in deep water represents the far offshore waves, and they are operated upon in a computer by factors that account for the effects of changing depth and reflection as the wave proceeds along a prescribed sloping beach, where the depth is known as a function of distance along the beach. The sum of all the constituent wave elements, each of which is treated by the parameters changing the amplitude, wave number, etc. as indicated previously, will then yield the complete wave form at various points along the beach. This can also be accomplished for exhibiting a spatial variation at a fixed time, for a series of time increments, thereby providing the wave pattern in a region as a function of time. This would be the "picture" of the waves as experienced by an observer moving through the waves on a boat.

The procedure to be used is indicated for the case of a wave of frequency ω_i , assuming that the wave propagates in a direction normal to the shoreline. The wave is observed from a boat assumed to travel normal to the shoreline, at a speed u , thereby representing a following sea. The origin of coordinates of the inertial frame is located at a point x_b distant from the shoreline, assuming a beach of constant slope α , and a water depth of h_0 at this offshore reference point. With the bottom contour given by

$$h = h_0 - \alpha x_0 \quad , \quad (34)$$

where $h_0 = \alpha x_b$, and an initial wave elevation at that point

(assumed to be in sufficiently deep water) given by

$$\eta_o = a_o \sin (k_o x_o - \omega_i t) \quad (35)$$

(observed at a stationary reference), the wave as seen by the moving observer on the boat is then

$$\eta_m = a_o D(\omega_i; h) \sin \left[k_i x + k_i \int_0^t u dt - \omega_i t \right] \quad (36)$$

In Equation (36) the observation point is chosen at a value of x measured relative to the boat, i.e. at a fixed distance from the CG of the craft; and other parameters such as k_i , D are dependent upon the local value of h at each instant of time, i.e.

$$h = h_o - \alpha \int_0^t u dt \quad (37)$$

as the boat progresses toward the beach. The quantity k_i is defined by

$$\frac{\omega_i^2}{g} = k_i \tanh k_i h \quad (38)$$

(as in Equation (3)), and D is given by Equation (2), so that the variation of these parameters as the boat moves and changes the local value of h is evident.

The process described above is carried out for as many other sinusoidal wave forms (at other frequencies) as desired to represent an offshore spectrum, and the results added together to produce a time history of the observed waves at a fixed point relative to the moving craft. With the reference offshore wavelength given by $\lambda_o = \frac{2\pi g}{\omega_m^2}$, where ω_m is the frequency of maximum

spectral energy, the wave pattern changes in the region near that defined in Equation (25) from an oscillatory type of wave to a solitary wave form. In order to insure continuity, the solitary wave crest follows the trough of the last oscillatory wave form in this "transition" region, with a continuous numerical transition weighting of the oscillatory-type waves and the complete solitary wave form. The height of the solitary wave form in this initial transition region is assumed to be equal to the significant wave height of the original offshore waves. A discussion of the computational technique for achieving this model of a solitary wave is presented in a later section of the report.

For the present problem, the wave field is evaluated in

terms of the inertial reference coordinate x_0 , which is measured from an initial origin at distance x_b from shore, where the x_0 -axis is perpendicular to the beach. The solitary wave propagates according to

$$\eta = H \operatorname{sech}^2 \left\{ \sqrt{\frac{3H}{4h^3}} \left(x + \int u dt - ct \right) \right\} \quad (39)$$

relative to the ship, for a following sea case, with x measured relative to the craft CG. The height change follows the relation given by Equation (27), with the depth variations as functions of time obtained from Equation (37). This continues until the limit condition for breaking given by Equation (26) is reached, after which the only effect remaining (after breaking) is the water elevation equal to the run-up R , which can be represented as an increased surface elevation, with a longitudinal velocity given by Equation (33).

For the head sea case, associated with retraction from the beach, the basic wave geometry variations in accordance with distance along the beach from the offshore reference point remain the same. The major change that occurs is in the argument of the sech function of the solitary wave representation, which becomes

$$\sqrt{\frac{3H}{4h^3}} \left[x_b - x - \int u dt - ct \right] \quad (40)$$

The wave heights, breaker forms, etc. associated with the wave system for this head sea case are obtained in the same manner as for the following sea case.

The establishment of the run-up elevation is made at the point of breaking, and this must be synchronized with the solitary waves at breaking to insure continuity and physical realism. This effect must also be re-initiated at each solitary wave breaking to provide the required periodicity. Methods of carrying out these operations on a digital computer are provided in a later section.

5. EQUATIONS OF MOTION

The equations of motion are written with respect to a moving axis system whose origin is at the ship CG. These equations represent the motion of the ship with six degrees of freedom, and it is assumed that there is a vertical center-line of symmetry, the ship mass and CG location are constant for any mode of operation, and that products of inertia are zero. For the present case of the assault boat, the equations are given by the following:

$$m(\dot{u}-vr+wq) = X \quad (41)$$

$$m(\dot{v}+ru-pw) = Y \quad (42)$$

$$m(\dot{w}-qu+pv) = Z \quad (43)$$

$$I_{xx}\dot{p} + qr(I_z - I_y) = K \quad (44)$$

$$I_{yy}\dot{q} + pr(I_x - I_z) = M \quad (45)$$

$$I_{zz}\dot{r} + pq(I_y - I_x) = N \quad (46)$$

The external forces and moments acting on the boat (indicated by the right hand sides of the equations above) arise from hull hydrodynamic and hydrostatic reactions; propeller effects; rudder deflection; control action; and aerodynamic reactions due to wind. These are represented as

$$F = F(\text{hull}) + F(\text{props}) + F(\text{rudders}) + F(\text{control}) \\ + F(\text{waves}) + F(\text{wind}) \quad (47)$$

and

$$M = M(\text{hull}) + M(\text{props}) + M(\text{rudders}) + M(\text{control}) \\ + M(\text{waves}) + M(\text{wind}) \quad (48)$$

in general form for the forces and moments.

The ship motions are referred to an inertial reference frame in order to determine the absolute position relative to the shoreline and/or an operating area offshore. The origin of the inertial reference frame is chosen to be located at an offshore point 1,000 yards from the beach, with the x_0 -axis directed normal to the shoreline, which is then parallel to the y_0 -axis. The main angle indicating orientation of the ship with respect to the inertial reference frame in the present case is the yaw angle ψ , since the roll and pitch angles are expected to be small. The inertial axis system and the body axes are related by (see [16]) the matrix transformation

$$\begin{bmatrix} x_0 \\ y_0 \\ z_0 \end{bmatrix} = \begin{bmatrix} B_{xx} & B_{xy} & B_{xz} \\ B_{yx} & B_{yy} & B_{yz} \\ B_{zx} & B_{zy} & B_{zz} \end{bmatrix} \begin{bmatrix} x \\ y \\ z \end{bmatrix} \quad (49)$$

where

$$\begin{aligned}
B_{xx} &= \cos \theta \cos \psi ; & B_{xy} &= \sin \phi \sin \theta \cos \psi - \cos \phi \sin \psi \\
B_{xz} &= \cos \phi \sin \theta \cos \psi + \sin \phi \sin \psi ; & B_{yx} &= \cos \theta \sin \psi \\
B_{yy} &= \sin \phi \sin \theta \sin \psi + \cos \phi \cos \psi & & (50) \\
B_{yz} &= \cos \phi \sin \theta \sin \psi - \sin \phi \cos \psi ; & B_{zx} &= -\sin \theta \\
B_{zy} &= \sin \phi \cos \theta ; & B_{zz} &= \cos \phi \cos \theta
\end{aligned}$$

For small values of ϕ and θ , with large yaw angle ψ possible, and retaining only linear terms, the relation becomes

$$\begin{bmatrix} x_o \\ y_o \\ z_o \end{bmatrix} = \begin{bmatrix} \cos \psi & -\sin \psi & \theta \cos \psi + \phi \sin \psi \\ \sin \psi & \cos \psi & \theta \sin \psi - \phi \cos \psi \\ -\theta & \phi & 1 \end{bmatrix} \begin{bmatrix} x \\ y \\ z \end{bmatrix} \quad (51)$$

In the present problem involving a ship on the surface, the heave motion is also small, and hence analysis of coupled heave and pitch can be refined to a fixed orientation axis system that translates with the body but does not rotate with the body. In that case the z-axis displacement for the body axis system, for the fixed orientation system, and also for the inertial system (z_o -axis) are identical, within linear theory, for the present purposes. The only relations between the coordinate frames are those concerned with horizontal plane displacements, and these navigation equations are then

$$\begin{aligned}
x_o &= x \cos \psi - y \sin \psi \\
y_o &= y \cos \psi + x \sin \psi
\end{aligned} \quad (52)$$

when the craft is proceeding toward shore, and

$$\begin{aligned}
x_o &= y \sin \psi - x \cos \psi \\
y_o &= -y \cos \psi - x \sin \psi
\end{aligned} \quad (53)$$

when the craft is retracting from the beach. An illustration of the relations between the inertial frame and the ship axis, when the ship is in either of these respective modes of operation, is shown in Figure 6. For the case where the boat is retracting from the beach, in a stern-first attitude, the body axis system on the boat is changed. In that case the x-axis is positive from the CG to the boat stern, and other axis orientations are similarly

changed. The yaw angle ψ , when measured from the inertial frame, is really $(180^\circ + \psi)$, with changes only considered relative to an imaginary axis parallel (but opposite) to the x_0 -axis, as indicated in Figure 6.

In the further derivation of the equations, it is assumed that the vertical plane motions of heave and pitch have negligible coupling with the lateral plane motions of yaw, sway, and roll. Similarly the effect of surge (i.e. forward speed variation) is coupled with the lateral plane motions, as well as with the vertical plane heave and pitch motions. These assumptions regarding relations between the variables allow simplification of the left hand sides of Equations (41)-(46) and in the evaluation of the various hull forces and moments. The various forms in the equations are obtained by analysis (see [2]) of the model test data in [1], and there are often significant differences in the equations for the two configurations considered, due to the reversal of the bow and stern aspect of the boat when it travels toward the beach and retracts seaward from the beach. In the resulting equations of motion the configurations will be identified as heavy and light, with the understanding that the light configuration applies to the retraction stern-first mode of operation.

On the basis of the preceding discussion, the equations of motion are simplified to

$$m(\dot{u} - vr) = X \quad (54)$$

$$m(\dot{v} + ru) = Y \quad (55)$$

$$m\dot{z} = Z \quad (56)$$

$$I_{xx}\dot{p} = K \quad (57)$$

$$I_{yy}\dot{q} = M \quad (58)$$

$$I_{zz}\dot{r} = N \quad (59)$$

In order to complete the general representation of the equations of motion, the following kinematic relations are included:

$$p = \frac{d\phi}{dt} = \dot{\phi} \quad (60)$$

$$q = \frac{d\theta}{dt} = \dot{\theta} \quad (61)$$

$$r = \frac{d\psi}{dt} = \dot{\psi} \quad (62)$$

where ϕ is the roll angle and θ the pitch angle.

6. HULL FORCES AND MOMENTS

The forces acting on the hull arise from both hydrodynamic and hydrostatic effects, where the hydrostatic effects are only included in the heave, pitch, and roll degrees of freedom, and manifest themselves as displacement-type terms. The hydrodynamic forces arise due to inertial, circulatory, and viscous effects due to interaction between the hull and the fluid. The forces are expressed as functions of the accelerations and velocities of the hull, and for the motions of surge, sway and yaw are generally represented in a Taylor series expansion. A number of terms are expected to be small on the basis of symmetry, and hence they are neglected, and the representation is primarily dominated by linear terms in the equations. This is due to the fact that only small angular changes will be made by the coxswain during the course of his motion toward and away from the beach, since he will always aim to keep the boat normal to the wave crests, and since extensive studies, e.g. [3], have shown that the motions of heave and pitch in waves are primarily linear.

The hull forces are represented in terms of a varying forward speed, since that quantity will be controlled during the course of different maneuvers. As a result certain nonlinear terms involving forward speed will appear in the equations, and these are primarily parametric in nature. The hydrodynamic forces due to hull motions are considered to be independent of propeller and rudder actions, and any effect on net forces is taken into account when considering those particular elements. Thus the axial hull force terms are limited in this section, since the data analysis [2] of the test results in [1] considered the net effect of thrust and resistance, which is treated in another section.

The equations for hull forces for the surge, sway and yaw modes are generally expressed as functions of the motion parameters representing the velocities and accelerations in these modes of motion. A Taylor series expansion is carried out up to second order in order to include nonlinear effects, and a typical example for the case of the lateral hull force is shown by

$$Y(u, v, r, \dot{u}, \dot{v}, \dot{r}) = Y_e + Y_u \Delta u + Y_v v + Y_r r + Y_{\dot{v}} \dot{v} + Y_{\dot{u}} \dot{u} + Y_{\dot{r}} \dot{r} + Y_{vu} v \Delta u + Y_{ru} r \Delta u \quad (63)$$

where the subscripts represent partial derivative operations, and the initial equilibrium condition (denoted by subscript e) is straight ahead motion at constant speed. Since there are no effects on the Y-force due to axial acceleration \dot{u} ; no lateral force exists in equilibrium; and the ship is almost symmetric fore-and-aft, a number of coefficients are zero (or negligible), i.e. $Y_e = Y_u = Y_{\dot{u}} = Y_{\dot{r}} = 0$. With the forward speed

being a total variable, no perturbation effects due to speed changes alone exist, and since (see [16])

$$\begin{aligned} Y_v &= \frac{\rho}{2} L^2 u Y'_v \\ Y_r &= \frac{\rho}{2} L^3 u Y'_r \end{aligned} \quad (64)$$

where Y'_v and Y'_r are measured nondimensional coefficients, all effects of forward speed and the variables v and r are incorporated therein, without the necessity of inclusion of any second order terms involving Δu (forward speed perturbation). As a result the lateral hull force is represented by

$$Y_{\text{hull}} = Y_v \dot{v} + Y_1 uv + Y_2 ur \quad (65)$$

where

$$Y_1 = \frac{\rho}{2} L^2 Y'_v, \quad Y_2 = \frac{\rho}{2} L^3 Y'_r \quad (66)$$

In a similar manner the hull yaw moment is represented by

$$N_{\text{hull}} = N_r \dot{r} + N_1 ur + N_2 r|r| + N_3 uv \quad (67)$$

where the $r|r|$ term in the yaw moment equation is included to allow for yaw damping effects at low forward speed, when turning around during retraction, or for hull forces to resist propeller thrust control actions when beached. The form of the hull reactions Y_{hull} and N_{hull} in Equations (65) and (67) is valid for both the heavy configuration and the light configuration, but different values of the coefficients will generally be present for each configuration.

The axial hull force expression, neglecting any resistance terms associated with purely axial motion (which are included together with net propulsive forces), is given by

$$X_{\text{hull}} = X_u \dot{u} + X_1 u|v| + X_2 vr \quad (68)$$

for the heavy configuration, and

$$X_{\text{hull}} = X_u \dot{u} + X_2 vr + X_3 v^2 \quad (69)$$

for the light configuration. The major difference between the two expressions is the form of the axial force variation due to sideslip angle, i.e. the $u|v|$ and v^2 terms, which occurs due to the manner of mathematical fit to the available experimental data (see [2]). The X_u term is the longitudinal added mass, and the $X_2 vr$ term occurs as a hydrodynamic inertial reaction, as indicated by potential flow dynamic equations in [17].

For roll motion the hull equations are governed by forces due to roll inertia, damping, and hydrostatic restoring effects. Coupling is known to exist with yaw and sway, with the main effect due to sway, while roll effects (due to the hull) on yaw and sway are generally negligible. A simplified model of hull roll moments, originally derived in [4], is used herein and allows for the coupling of sway in modifying the resulting coefficients in the roll equation. Thus the hull roll moment representation is given by

$$K_{\text{hull}} = K_p \ddot{\phi} + K_p \dot{\phi} - W|GM|\phi \quad (70)$$

where W is the total weight (displacement) and $|GM|$ is the metacentric height.

When analyzing roll, and also for heave and pitch, which are the primary wave-influenced motions due to their hydrostatic restoring terms, the equations are usually written with respect to an axis system that translates with the body, but with a fixed orientation, i.e. they do not rotate with the body. Since these motions are linear, and do not couple with the other motions in a nonlinear manner, they can be treated in their usual manner without any loss of generality in the complete six degree of freedom equations. In the derivation of the equations for heave and pitch, the boat is assumed to be a symmetrical rectangular block of beam B , length $2l$, and draft d , with the CG (origin of coordinates) assumed to be at the geometric center (axially) and the value of the draft selected as an average that provides the correct total displacement ($d = 2.7$ ft. for the heavy condition and $d = 1.4$ ft. for the light load). This procedure is sufficiently accurate for representing the hull forces and moments, allowing simplification due to symmetry for these terms as well as for the wave-induced forces (to be discussed in a later section).

With the positive direction of z downward, the derivation of the local inertial hydrodynamic vertical force at a section is obtained from the simplified result of slender-body theory [18], which states that the local force on any section is equal to the negative time rate of change of fluid momentum. This is expressed by

$$\frac{dz_i}{d\xi} = - \frac{D}{Dt} \left[A'_{33} w_b \right] \quad (71)$$

where the time derivative operation is defined by

$$\frac{D}{Dt} = \frac{\partial}{\partial t} + u \frac{\partial}{\partial \xi} \quad (72)$$

A'_{33} is the vertical added mass (two-dimensional) of the cross-section, and w_b is the section vertical velocity (along z -direction, i.e. positive down) given by

$$w_b = \frac{D}{Dt} (z - \xi\theta) = \dot{z} - \xi\dot{\theta} + u\theta \quad (73)$$

In the above equations the coordinate ξ is a "dummy" variable along the longitudinal body coordinate x , and coincident with it. Since the boat is assumed to be a uniform rectangular block,

the value of A'_{33} is constant at every section and $\frac{dA'_{33}}{d\xi} = 0$ except at the ends, where it has δ -function form. Expanding the operation of Equation (71) and integrating over the hull yields

$$z_i = - \int_{-l}^l A'_{33} d\xi \cdot \dot{z} - u \int_{-l}^l A'_{33} d\xi \cdot \dot{\theta} \quad (74)$$

where the symmetry condition $\int_{-l}^l A'_{33} \xi d\xi = 0$ is invoked.

The damping force in heave arises due to energy dissipation associated with wave generation by the ship motions on the free surface. The ratio of the amplitude of the heave-generated two-dimensional waves to the heave motion amplitude of a section is denoted as \bar{A}_z , and by equating the energy balance between ship work and outgoing wave energy, the vertical damping force per unit vertical velocity of the section is expressed as

$$N'_{zz} = \frac{\rho g^2 \bar{A}_z^2}{\omega_e^3} \quad (75)$$

where ω_e is the circular frequency of oscillation (usually frequency of encounter for ship motions). The vertical damping force at each section is then

$$\frac{dz_d}{dx} = - N'_{zz} (\dot{z} - \xi\dot{\theta} + u\theta) \quad (76)$$

and the total vertical damping force is determined by integrating over the ship length, leading to

$$z_d = - \int_{-l}^l N'_{zz} d\xi \cdot \dot{z} - u \int_{-l}^l N'_{zz} d\xi \cdot \theta \quad (77)$$

and applying symmetry, since N'_{zz} is constant for each section.

The hydrostatic restoring force due to static vertical displacement (on a calm free surface) of a ship section is

$$\frac{dZ_h}{d\xi} = - \rho g B^* (z - \xi \theta) \quad , \quad (78)$$

leading to a total force given by

$$Z_h = - \rho g \int_{-l}^l B^* d\xi \cdot z = - 2\rho g l B \cdot z \quad , \quad (79)$$

since $B^* = B$ is constant for each section.

The pitch moment terms corresponding to all the force terms derived in the foregoing are easily obtained by use of the relation

$$\frac{dM}{d\xi} = - \xi \frac{dZ}{d\xi} \quad , \quad (80)$$

followed by the required integrations over the hull. This leads to

$$M_i = - \int_{-l}^l A'_{33} \xi^2 d\xi \cdot \ddot{\theta} + u \int_{-l}^l A'_{33} d\xi \cdot \dot{z} + u^2 \int_{-l}^l A'_{33} d\xi \cdot \theta \quad (81)$$

$$M_d = - \int_{-l}^l N'_{zz} \xi^2 d\xi \cdot \dot{\theta} \quad , \quad (82)$$

$$M_h = - \rho g \int_{-l}^l B^* \xi^2 d\xi \cdot \theta = - \frac{2}{3} \rho g B l^3 \cdot \theta \quad (83)$$

The added mass and damping coefficients, A'_{33} and N'_{zz} , appearing in the preceding equations are functions of the geometry of the ship section (which is assumed constant in the present case for treating heave and pitch) and are also functions of frequency. They are determined from solution of a hydrodynamic free surface boundary value problem for a class of representative ship sections, as shown by the results in [19]. In order to allow a simple representation of the equations, an approximation is made in selecting constant values for these terms which are independent of frequency, with these constants selected in a manner so that the basic dynamic characteristics of this system are properly exhibited. Since the hydrostatic

restoring terms are constant, the selection of the added mass is such that the natural periods in heave and pitch are close to those observed experimentally. Similarly the damping values are chosen at values appropriate to the range of frequencies that are anticipated for the assault boat when it approaches the beach or when retracting. As a result of the different displacements associated with these two operations, and the expected range of speeds in each case, a different set of constant coefficients is determined for the two ship configurations. An outline of the basis for selection of these values is provided in [2]. Similar reasoning is applied to the determination of the added roll inertia, while the roll damping is determined from combined theory and empirical data. Reference [2] provides the detailed information on the determination of these parameters in accordance with this procedure.

In the course of the hydrodynamic force representations developed above, certain assumptions have been made that were not delineated in detail, and they are described by the following. Hydrodynamic forces due to inertia asymmetries, which were explicitly neglected in the case of heave and pitch, have also been neglected in the representation of the lateral force and yaw moment. In particular the stability derivative terms Y_r and N_v (in conformity with SNAME notation [16]) have been assumed to be zero and have been deleted from the listings in Equations (65) and (67). Another assumption made is the lack of any influence of the varying depth, along the sloping beach, on the values of the coefficients included in the previous equations. Measurements made in [20] have indicated only small variations in lateral motion hydrodynamic coefficients (yaw and sway), within the range of variation considered significant in comparison with other contributory factors such as frequency and forward speed. Thus it is assumed herein that constant values exist for these coefficients, and that the varying shallow water influence is negligible. Since average constant coefficients have been selected for the force terms for heave, pitch, and roll, a similar neglect of such effects is inherent in the equations. The force expression that is known to vary significantly as the depth changes is the axial force, and data pertinent to that variation was obtained in [1] and analyzed for use in the present report in [2]. This data will be discussed while considering propeller effects, since the net axial force is the quantity of importance for the equations in this program.

7. PROPELLER FORCES

The LCM (6) is a twin-screw propeller craft, with both propellers being right-handed [5]. These propellers have three blades, with 2 ft. diameters, and are described in [6]. The propeller effects acting on the assault boat only produce an axial force (along x-axis), a lateral force (along y-axis), and a yawing moment (about z-axis). The present section treats the case where both propellers are operating in unison to propel the craft, and any considerations of differential propeller

action are treated in the section concerned with control effects, where such control effects are due to the action of the coxswain via his control of the propellers (rudder control is considered separately, in another section). From the tests in [1], as analyzed by the procedures in [2], information was obtained on the variation of the net axial force, i.e. T-R, the difference between thrust and resistance, for a range of ship speeds and propeller rpm values. This data allowed determination of the axial force as a function of ship longitudinal speed and propeller rotational speed, and also provided data for determination of the self-propulsion conditions, i.e. the speed corresponding to a particular propeller rotational speed for twin screw operation. The tests carried out under self-propulsion conditions then provided information on the side force and yawing moment associated with propeller operation under these conditions, from which a mathematical form was fit in order to provide expressions for use in the present mathematical model. Self-propulsion information is presented for the two configurations in Figures 7 and 8, where the rpm data is for propeller rpm. Since there is a reduction gear, with ratio 1.51, employed on this vehicle [21], the engine rpm is increased by that magnitude. This data is applicable only to deep water conditions for each case.

Since the propellers are right-handed, a starboard side force and a yawing moment to port are obtained for forward operation. (heavy configuration) and these terms are represented by

$$Y_{(\text{props})} = -7.13 u + 5.74 u^2 - 0.75 u^3 + 0.03 u^4 \quad (84)$$

$$N_{(\text{props})} = 103.13 u - 114.2 u^2 + 15.61 u^3 - 0.75 u^4 \quad (85)$$

which are only functions of the forward speed (any influence of rpm is inherently contained within the speed variation, since there is a unique rpm for a given speed under normal twin-screw operation). Similarly the side force and yawing moment for astern operation (light configuration) are given by

$$Y_{(\text{props})} = 6.91 u + 0.58 u^2 \quad (86)$$

$$N_{(\text{props})} = 156.91 u + 15.78 u^2 \quad (87)$$

where the axis orientation for this condition is indicated in Figure 6. It is this effect of a lateral force and yaw moment due to similar rotational directions of the twin propellers that causes coursekeeping difficulty for this craft.

The net longitudinal force acting on the craft as a function of forward speed and propeller rpm is found by obtaining a "collapsed" form of the data, in the same manner as the ordinary thrust coefficient parameter $K_T = \frac{T}{\rho n^2 D^4}$

for a propeller is represented. The resultant form is somewhat complicated due to the wide range of speeds in this program, especially for the forward motion of the heavy configuration. The force expression for the heavy configuration is given by

$$X_{(props)}^{(1)} = 4.93 n_o^2 + 0.82 u^{3/2} n_o - 0.06 u^3, \quad (88)$$

where n_o = operating propeller rotational rate (rps). This expression is found by means of fitting the data with a mathematical expression, after obtaining the collapsed form for the range of operating forward speed and propeller rotational speed (see [2]). The operating propeller rotational rate n_o is defined by

$$n_o = \frac{1}{2} (n_p + n_s), \quad (89)$$

which is the mean of the port and starboard propeller rates. When both propellers are operating in unison at the same rate the value of n_o is proper, as required in the present section, and any effect of different propeller rates (port and starboard) is considered when treating control forces. The relation in Equation (88) is valid for the case of motion in deep water, where no influence of the shallow depth is present. The effect of motion along a beach where the depth is decreasing results in an increased resistance, which is found (by mathematical fit, see [2]) to be represented in the form

$$X_{(props)}^{(2)} = 0.08 u n_o^2 - 77.37 \frac{u^2 n_o \alpha}{h} \quad (90)$$

where h is the local depth at the ship CG and α is the beach slope. The sum of the two expressions in Equations (88) and (90) is the axial force appropriate to the operation of the heavy configuration when approaching a shoreline.

Similar results are found for the case of the light configuration, where the deep water axial force is represented by

$$X_{(props)}^{(1)} = 16.36 n_o^2 - 17.97 u n_o - 3.38 u^2 \quad (91)$$

and the effect of shallow depth is given by

$$X_{(props)}^{(2)} = 0.11 u n_o - 62.86 \frac{u^2 n_o \alpha}{h} \quad (92)$$

8. RUDDER FORCES

The effect of rudder deflection produces a side force, yawing moment and axial force. The LCM (6) has twin rudders that deflect together in unison. The rudders lie in the wake of the propellers when the assault boat moves forward in the heavy configuration, while they are ahead of the propellers in the light configuration associated with the retraction operation. Thus the forces and moments from the rudders depend upon the rudder angle, the longitudinal ship speed, and the propeller rotational speed, with less dependence on the propeller speed for the light configuration. The experimental data obtained in [1] was analyzed to obtain data on the rudder forces, which were found to depend upon forward speed when represented in the form

$$Y_{\text{(rudders)}} = Y'_{\delta} \frac{\rho}{2} L^2 u^2 \delta \quad (93)$$

$$N_{\text{(rudders)}} = N'_{\delta} \frac{\rho}{2} L^3 u^2 \delta \quad (94)$$

and this dependence can then be ascribed to the effect of the propellers. The hydrodynamic derivatives Y'_{δ} and N'_{δ} depend upon forward speed, and are given by

$$Y'_{\delta} = 0.00093 u \quad (95)$$

and

$$N'_{\delta} = -0.00036 u \quad (96)$$

for the heavy condition, and by

$$Y'_{\delta} = 0.00016 u \quad (97)$$

and

$$N'_{\delta} = 0.000078 u \quad (98)$$

for the light condition. The notations, positive direction of rotation, etc. used here are in conformity with [16]. The final representation of the lateral force and yaw moment for rudder deflection is then given by

$$Y_{\text{(rudders)}} = 2.71 u^3 \delta \quad (99)$$

and

$$N_{\text{(rudders)}} = -56.69 u^3 \delta \quad (100)$$

for the heavy configuration, and by

$$Y_{\text{(rudders)}} = 0.47 u^3 \delta \quad (101)$$

and

$$N_{\text{(rudders)}} = 12.28 u^3 \delta \quad (102)$$

for the light configuration.

Operational experience has shown that the rudders are not very effective in controlling this craft when it is moving astern (retraction conditions), and hence the rudder forces are not significant in comparison to the other forces acting upon the ship, at the low speed associated with this condition [5]. As a result, extensive control action is obtained by means of controlling the propeller thrust in a differential manner, and the rudder effects are only additional to this main method of control for this operational condition. The relations provided in this section are assumed to be valid for rudder angles in the range up to $\pm 30^\circ$, where linear behavior is still a valid approximation for the lateral force and moment (see [2]).

Some consideration was also given to an alternate representation of the rudder forces in a manner more dependent upon propeller rotational rate, rather than forward speed alone. While such a relation was obtained (see [2] for details), the present form in Equations (99)-(102) is retained herein since it is anticipated that the rudders will primarily be used during ahead motion of the heavy configuration at appreciable forward speeds. The representation in terms of propeller rotational speed (for the heavy configuration) is useful in low speed operations where propeller-rudder interaction could produce turning action on the craft, and that form is presented in [2] in case a particular situation arises where such an expression would be more useful in certain simulation exercises.

The rudder deflection will also produce an additional resistance, resulting in an axial force proportional to δ^2 . This force is expected to be small, and hence an approximate representation is given by

$$X_{(\text{rudders})} = -2.8 u^2 \delta^2 \quad (103)$$

which is obtained by analytical estimation in [2].

Due to the small size of the rudders, and the direct manual control exercised by the coxswain, very little time lag exists in actuating the rudder to a commanded value. A simple analysis, based on considerations ordinarily used in treating such effects [22], shows a time lag of less than 1 second ($\approx .3$ sec. for a 10 knot forward speed) so that such effects are neglected in this report.

9. CONTROL FORCES

As indicated previously, control forces are obtained by use of differential thrust of the propellers, under command of the coxswain. While it is known that the lateral force and yaw moment effects of a single propeller are not the same, when considering the separate forces exerted by either the port or starboard propeller acting alone (see the results in [1] and

discussion in [2]), the separate thrust force effects of each propeller can be considered to act independently of each other, as a first assumption. Thus it is possible to represent these effects using data on propeller thrust characteristics alone as obtained in [1], with the assumption that equal thrusts are developed by each propeller, at the same forward speed and rotational speed, when operating together in a twin-screw installation.

Measurements of the propeller thrust, under twin-screw action, were obtained in [1] and analyzed in [2]. It was found that the total thrust under these conditions, in ahead operation for the heavy configuration, can be represented by

$$T = 13.44 n_o^2 \quad (104)$$

Similarly the total thrust under twin-screw operation, for the light configuration moving stern first, is given by

$$T = 0.95 n_o^3 \quad (105)$$

These results are appropriate to the "normal" operating condition of the boat when moving ahead with twin-screw operation in unison, and it is assumed that half of the total thrust is developed by each propeller.

When considering differential thrust action, a rotational speed different from the normal operating value referred to above is selected by the coxswain, and the change in thrust for the port or starboard propeller (based upon the reference to these locations when considering the boat in its normal bow-first ahead operation) can be represented by

$$\Delta T_{p,s} = \frac{1}{2} [T(n_{p,s}) - T(n_o)] \quad (106)$$

where

$$n_{p,s} = \text{rps of port or starboard propeller,} \\ \text{as selected by the coxswain for} \\ \text{differential action} \quad (107)$$

and n_o is defined in Equation (89). The effect of this altered thrust generated by the propellers is a yawing moment due to the location of each propeller at a distance of 2.5 ft. from the longitudinal centerline given by

$$N_{(\text{control})_p} = 1.25 [T(n_p) - T(n_o)] \quad (108)$$

for the action of the port propeller, and

$$N_{(\text{control})_s} = -1.25 [T(n_s) - T(n_o)] \quad (109)$$

for the action of the starboard propeller, when applied to the heavy configuration in normal forward motion. The resulting total control yaw moment is the sum of these expressions, given by

$$N_{(\text{control})} = 1.25 \left[T(n_p) - T(n_s) \right] \quad (110)$$

which only depends upon the values of the port and starboard propeller rotational speeds. Similarly, for the light configuration appropriate to retraction conditions, the yawing moment due to differential propeller control is given by

$$N_{(\text{control})} = 1.25 \left[T(n_s) - T(n_p) \right] \quad (111)$$

The effect of any change in either propeller rotational speed on the axial force is manifested by the use of the resulting value of the operating propeller speed n_o (defined in Equation (89)), in the expressions given by Equations (88), (90)-(92).

Since the relatively small engines of the LCM (6) are under the direct control of the coxswain by means of hand throttles, it is expected that rapid response to commanded settings of the engine will occur. Thus the resulting propeller rotational speed will respond rapidly, and for the purposes of this report the lags will be considered to be negligible. Since the propeller force effects due to changing propeller speed will produce relatively small accelerations on the boat, any effects due to neglecting the small time lag are still expected to result in smooth motion outputs.

10. WAVE EXCITING FORCES AND MOMENTS

The wave-induced forces and moments acting on the assault boat are made up of hydrostatic terms due to periodic buoyancy alterations as the waves progress past the ship hull, and hydrodynamic forces due to inertial effects of the wave velocities and accelerations acting at each ship section. The buoyancy effect for the vertical force is represented by

$$\frac{dZ^{(1)}}{d\xi}(\text{waves}) = -\rho g B^* \eta(\xi, t) \quad (112)$$

at each section, and the inertial contribution to the wave exciting forces may generally be represented by

$$\frac{dF}{d\xi}(\text{waves}) = \frac{D}{Dt} (A'_{ii} V_{oi}) + \rho S \frac{D}{Dt} V_{oi} \quad (113)$$

where A'_{ii} is a particular local added mass term, $S = B \cdot d$ is the sectional area, and V_{oi} is a component of the wave orbital

velocity evaluated at the undisturbed surface along the ship vertical centerline. The waves are generally assumed to be propagating in a direction relative to the ship hull defined by the angle γ , where γ is the angle between the ship x-axis and the normal to the wave crests. For the present case the angle γ is defined by

$$\gamma = \psi - \beta \quad (114)$$

where β is the angle made by the normal to the wave crests, measured relative to the x_0 -axis, which changes as the shoreline is approached due to refraction effects.

The surface wave elevation relative to the ship is represented by

$$\eta = a \sin \left[k \xi \cos \gamma + k y \sin \gamma - \omega t + k \cos \gamma \int_0^t u dt \right] \quad (115)$$

in terms of the dummy variable ξ along the ship x-axis, where the amplitude a changes as the boat approaches the shore in accordance

with Equation (5) (a term involving $\int_0^t v dt$ has been neglected in

Equation (115) as its influence is not significant for wave forces). The wave orbital velocities along the x, y, and z-axes are defined as

$$u_0 = a\omega \coth kh \cos \gamma \sin \left(k\xi \cos \gamma - \omega t + k \cos \gamma \int_0^t u dt \right) \quad (116)$$

$$v_0 = a\omega \coth kh \sin \gamma \sin \left(k\xi \cos \gamma - \omega t + k \cos \gamma \int_0^t u dt \right) \quad (117)$$

$$w_0 = a\omega \cos \left(k\xi \cos \gamma - \omega t + k \cos \gamma \int_0^t u dt \right) \quad , \quad (118)$$

where they are evaluated at the mean free surface level along the ship centerline, $y = 0$. The orbital accelerations, which are required in evaluating the wave forces according to Equation (113) are obtained by carrying out the operation

$$\frac{D}{Dt} = \frac{\partial}{\partial t} - u \frac{\partial}{\partial \xi} \quad (119)$$

and they are given by

$$\dot{u}_0 = -agk \cos \gamma \cos (k \xi \cos \gamma - f(t)) \quad (120)$$

$$\dot{v}_0 = -agk \sin \gamma \cos (k \xi \cos \gamma - f(t)) \quad (121)$$

$$\dot{w}_0 = a\omega^2 \sin (k \xi \cos \gamma - f(t)) \quad (122)$$

where $f(t) = \omega t - k \cos \gamma \int_0^t u \, dt$. (123)

The wave force in the z-direction due to hydrostatic effects, as indicated by Equation (112), is given by

$$\begin{aligned} Z_{(waves)}^{(1)} &= -\rho g a B \int_{-\ell}^{\ell} \sin (k \xi \cos \gamma - f(t)) \, d\xi \\ &= -2\rho g a B \int_0^{\ell} \cos (k \xi \cos \gamma) \, d\xi \cdot \sin f(t) \\ &= -2\rho g a B \frac{\sin (k \ell \cos \gamma)}{k \cos \gamma} \sin f(t) \end{aligned} \quad (124)$$

where symmetry considerations have been applied. The inertial hydrodynamic contribution to this force, according to Equation (113), is then found to be

$$\begin{aligned} Z_{(waves)}^{(2)} &= \left[2(\rho B d + A'_{33}) a\omega^2 \frac{\sin (k \ell \cos \gamma)}{k \cos \gamma} \right. \\ &\quad \left. + 2a\omega u A'_{33} \sin (k \ell \cos \gamma) \right] \sin f(t) \end{aligned} \quad (125)$$

where the δ -function behavior of the added mass at the ends is accounted for in the last term in this expression. With the pitch moment related to the vertical force in accordance with Equation (80), it can be shown that the results for the total wave-induced pitch moment are

$$\begin{aligned}
 M_{(\text{waves})} = & \left\{ 2\rho g a B \left[\frac{\sin(k \ell \cos \gamma)}{(k \cos \gamma)^2} - \frac{\ell \cos(k \ell \cos \gamma)}{k \cos \gamma} \right] \right. \\
 & - 2(\rho B d + A'_{33}) a \omega^2 \left[\frac{\sin(k \ell \cos \gamma)}{(k \cos \gamma)^2} - \frac{\ell \cos(k \ell \cos \gamma)}{k \cos \gamma} \right] \\
 & \left. - 2a \omega u A'_{33} \ell \cos(k \ell \cos \gamma) \right\} \cos f(t) \quad (126)
 \end{aligned}$$

The axial and lateral forces due to waves, in accordance with Equations (113), (116), and (117), are then given by

$$X_{(\text{waves})} = - 2\rho g a B d \sin(k \ell \cos \gamma) \cos f(t) \quad (127)$$

and

$$\begin{aligned}
 Y_{(\text{waves})} = & - \left[2(\rho B d + A'_{22}) a g \frac{\sin(k \ell \cos \gamma)}{\cos \gamma} \right. \\
 & \left. + 2a \omega \coth kh u A'_{22} \sin(k \ell \cos \gamma) \right] \cdot \sin \gamma \cos f(t) \quad (128)
 \end{aligned}$$

where A'_{22} is the lateral sectional added mass of the rectangular block representing the craft. From Equations (113) and (128) the yawing moment due to waves, defined by

$$\frac{dN_{(\text{waves})}}{d\xi} = \xi \frac{dY_{(\text{waves})}}{d\xi} \quad (129)$$

is then given by

$$\begin{aligned}
 N_{(\text{waves})} = & - \left\{ 2(\rho B d + A'_{22}) \frac{a g}{\cos \gamma} \left[\frac{\sin(k \ell \cos \gamma)}{k \cos \gamma} - \ell \cos(k \ell \cos \gamma) \right] \right. \\
 & \left. + 2a \omega \coth hk u A'_{22} \ell \cos(k \ell \cos \gamma) \right\} \sin \gamma \cdot \sin f(t) \quad (130)
 \end{aligned}$$

With the simplified form of roll moments due to the hull given by Equation (70), the roll moment due to waves can be represented by

$$K_{(\text{waves})} = \rho g a k \sin \gamma |GM| \int_{-\ell}^{\ell} S \cos (k \xi \cos \gamma - f(t)) d\xi$$

$$= 2\rho g a \tan \gamma |GM| B d \sin (k \ell \cos \gamma) \cos f(t) \quad , \quad (131)$$

which is based on a simplification of the wave-induced roll moment, as shown in [4]. This result is sufficiently accurate for use in the present study where roll is not a predominant motion of concern.

In all of the preceding results, the application has been made to oscillatory waves propagating toward a shoreline, and the magnitude of the associated parameters such as the wave amplitude, wavelength, etc. will vary in accordance with the position of the craft along the sloping beach (i.e. as a function of the local depth h). The force and moment magnitudes depend upon the angle γ , but during the course of approaching a beach the coxswain often steers so that the boat tends to be normal to the crests, resulting in a small value of the angle γ . Some simplifications may be made, depending upon the magnitudes of γ expected in accordance with the initial heading direction of waves far offshore, so that the approximations $\cos \gamma = 1$ and $\sin \gamma \approx \gamma$ can be applied in some cases.

The results above are in a form that is primarily applicable to the case of following seas, when approaching the beach. Application to the head sea case, corresponding to retraction when returning seaward, is made by the appropriate change in the definition of the function $f(t)$ to

$$f(t) = \omega t + k \cos \gamma \int_0^t u dt \quad (132)$$

changing its sign wherever it appears. The resulting change is a change in sign of the $Z_{(\text{waves})}$ and $N_{(\text{waves})}$ expressions, and also a change in the expression for the surface wave elevation. These changes are necessary as a result of the change in body axis orientations for the two operating conditions, as indicated in Figure 6, and they will produce consistent results for the motions with proper phase relations maintained.

Another important wave force necessary for this investigation is the added resistance due to waves, which is a nonlinear phenomenon. Considerations have only been given to determining the mean value of this force, and no simple expression exists

for theoretical evaluation of either the mean value or the total time variation of this term. Since prior experimental work [23] has indicated a proportionality of this force with the square of the wave amplitude for regular waves, a model for this added resistance is formulated as

$$X_{(\text{waves})}^{(2)} = -A \left\{ \eta \right\}^2 \quad (133)$$

where the $\left\{ \eta \right\}$ symbol represents the envelope of the encountered wave time history (at the ship CG). The envelope of a function is obtained by a full wave rectifying operation (i.e. absolute value of the function), followed by a low-pass filter, and the resultant function produced by the operations of Equation (133) will be slowly varying, with some higher frequencies (of small magnitude) superposed on the main modulating curve. Since the motion in head seas is known to produce the largest added resistance, the coefficient values (i.e. A values) in Equation (133) should reflect the difference between head and following sea results for the two configurations. For the following sea case (heavy configuration) the expression for this force is

$$X_{(\text{waves})}^{(2)} = -700 \left\{ \eta \right\}^2 \quad (134)$$

and for the light configuration, in head seas, it is

$$X_{(\text{waves})}^{(2)} = -300 \left\{ \eta \right\}^2 \quad (135)$$

A discussion of the choice of these values and their relation to observed craft behavior in model tests is given in [2].

Since the waves change form as they progress toward the shore, and are represented by solitary waves in the present approximate procedure, the wave forces acting on the ship will also change their form. The expressions for the wave forces due to a solitary wave are obtained by the same procedure as in [24], together with other hydrodynamic effects not included in [24]. The wave forces derived in [24] only consider forces for determining surge, heave, and pitch motions, and they are derived on the basis of the Froude/Kriloff hypothesis that neglects interaction between the wave and the ship (i.e. using the pressures existing in the wave field without allowing any modification due to the presence of the ship). The hydrodynamic inertial effects in waves, represented by Equation (113), provide additional force components for those modes and also allow extension of the results of [24] to provide wave force and moment expressions for the other three motions not considered in [24].

Using the results presented in [11] for the solitary waves, based upon the wave form expression given in Equation (39) for following seas, the water particle velocities evaluated at the still water level along the ship centerline are

$$\frac{u_o}{\sqrt{gh}} = \frac{H}{h} \cos \gamma \operatorname{sech}^2 \left\{ \sqrt{\frac{3H}{4h^3}} \left[x \cos \gamma - ct + \cos \gamma \int u dt \right] \right\} \quad (136)$$

$$\frac{v_o}{\sqrt{gh}} = \frac{H}{h} \sin \gamma \operatorname{sech}^2 \left\{ \sqrt{\frac{3H}{4h^3}} \left[x \cos \gamma - ct + \cos \gamma \int u dt \right] \right\} \quad (137)$$

$$\begin{aligned} \frac{w_o}{\sqrt{gh}} = & -\sqrt{3} \left(\frac{H}{h} \right)^{3/2} \operatorname{sech}^2 \left\{ \sqrt{\frac{3H}{4h^3}} \left[x \cos \gamma - ct + \cos \gamma \int u dt \right] \right\} \\ & \cdot \tanh \left\{ \sqrt{\frac{3H}{4h^3}} \left[x \cos \gamma - ct + \cos \gamma \int u dt \right] \right\} \end{aligned} \quad (138)$$

along the x, y, and z-axes of the ship, where c is defined in Equation (29). These results are generalizations for a heading between ship and wave, for a moving reference point, with the elevation of the solitary wave (along the ship centerline, $\gamma = 0$) represented by

$$\begin{aligned} \eta &= H \operatorname{sech}^2 \left\{ \sqrt{\frac{3H}{4h^3}} \left[x \cos \gamma - ct + \cos \gamma \int u dt \right] \right\} \\ &= H \operatorname{sech}^2 \left\{ \sqrt{\frac{3H}{4h^3}} \left[x \cos \gamma - g(t) \right] \right\} \end{aligned} \quad (139)$$

where

$$g(t) = ct - \cos \gamma \int u dt \quad (140)$$

The hydrostatic pressure at any depth in a solitary wave region is

$$p = \rho g (\eta + z_o) \quad (141)$$

where z_o is the depth below the undisturbed free surface level.

The time-dependent part of the pressure is $\rho g \eta$, and this quantity is used to derive the wave forces in [24]. Generalizing the result in [24] to the present case results in

$$X_{(waves)}^{(1)} = -\rho g B d H \left\{ \begin{aligned} & \operatorname{sech}^2 \epsilon \left[\ell \cos \gamma - g(t) \right] \\ & - \operatorname{sech}^2 \epsilon \left[\ell \cos \gamma + g(t) \right] \end{aligned} \right\} \quad (142)$$

for the longitudinal force in a solitary wave, where

$$\epsilon = \sqrt{\frac{3H}{4h^3}} \quad (143)$$

The vertical force in a solitary wave, from [24] is given by

$$Z_{(waves)}^{(1)} = -\frac{\rho g B H}{\epsilon} \left\{ \begin{aligned} & \tanh \epsilon \left[\ell \cos \gamma - g(t) \right] \\ & + \tanh \epsilon \left[\ell \cos \gamma + g(t) \right] \end{aligned} \right\} \quad (144)$$

and the pitch moment by

$$M_{(waves)}^{(1)} = \frac{\rho g H B \ell}{\epsilon} \left\{ \begin{aligned} & \tanh \epsilon \left[\ell \cos \gamma - g(t) \right] \\ & - \tanh \epsilon \left[\ell \cos \gamma + g(t) \right] \end{aligned} \right\} \\ + \frac{\rho g H B}{\epsilon^2} \log \left\{ \frac{\cosh \epsilon \left[\ell \cos \gamma + g(t) \right]}{\cosh \epsilon \left[\ell \cos \gamma - g(t) \right]} \right\} \\ - \frac{1}{2} \rho g B d^2 \left\{ \begin{aligned} & \operatorname{sech}^2 \epsilon \left[\ell \cos \gamma - g(t) \right] \\ & - \operatorname{sech}^2 \epsilon \left[\ell \cos \gamma + g(t) \right] \end{aligned} \right\} \quad (145)$$

The results for the wave forces in Equations (144) and (145) are due to hydrostatic effects, while the longitudinal force is also interpreted in that way. Additional terms due to hydrodynamic inertial effects exist for the vertical force and pitch moment, while these hydrodynamic terms are the only proper means for determining the lateral force and yawing

moment due to waves. The roll moment is found to be primarily determined by hydrostatic effects, after elimination of cross-coupling hydrodynamic terms in the equations of motion (see [4]), and the influence of hydrodynamic interaction for the longitudinal wave force is small due to the small longitudinal added mass of the boat relative to its physical mass.

Assuming that the relation in Equation (113) can be applied to the present shallow water case with a solitary wave representation, the wave force components due to this hydrodynamic effect are given below as

$$\begin{aligned}
 z^{(2)} = & \sqrt{3gh} \left(\frac{H}{h} \right)^{3/2} \left[\frac{(\rho B d + A'_{33}) c}{\cos \gamma} - A'_{33} u \right] \cdot \left\{ \text{sech}^2 \epsilon \left[\ell \cos \gamma - g(t) \right] \right. \\
 & \cdot \tanh \epsilon \left[\ell \cos \gamma - g(t) \right] + \text{sech}^2 \epsilon \left[\ell \cos \gamma + g(t) \right] \\
 & \left. \cdot \tanh \epsilon \left[\ell \cos \gamma + g(t) \right] \right\} \quad (146)
 \end{aligned}$$

$$\begin{aligned}
 M^{(2)} = & - \sqrt{3gh} \left(\frac{H}{h} \right)^{3/2} c \frac{(\rho B d + A'_{33})}{\cos \gamma} \cdot \left\{ \ell \text{sech}^2 \epsilon \left[\ell \cos \gamma - g(t) \right] \right. \\
 & \cdot \tanh \epsilon \left[\ell \cos \gamma - g(t) \right] - \ell \text{sech}^2 \epsilon \left[\ell \cos \gamma + g(t) \right] \\
 & \cdot \tanh \epsilon \left[\ell \cos \gamma + g(t) \right] + \frac{1}{2\epsilon \cos \gamma} \text{sech}^2 \epsilon \left[\ell \cos \gamma - g(t) \right] \\
 & \left. - \frac{1}{2\epsilon \cos \gamma} \text{sech}^2 \epsilon \left[\ell \cos \gamma + g(t) \right] \right\} + \sqrt{3gh} \left(\frac{H}{h} \right)^{3/2} A'_{33} \ell u \cdot \\
 & \left\{ \text{sech}^2 \epsilon \left[\ell \cos \gamma - g(t) \right] \cdot \tanh \epsilon \left[\ell \cos \gamma - g(t) \right] \right. \\
 & \left. - \text{sech}^2 \epsilon \left[\ell \cos \gamma + g(t) \right] \cdot \tanh \epsilon \left[\ell \cos \gamma + g(t) \right] \right\} \quad (147)
 \end{aligned}$$

$$\begin{aligned}
 Y_{(\text{waves})} = & - \frac{H}{h} \sqrt{gh} c \tan \gamma (\rho B d + A'_{33}) \cdot \left\{ \text{sech}^2 \epsilon \left[\ell \cos \gamma - g(t) \right] \right. \\
 & \left. - \text{sech}^2 \epsilon \left[\ell \cos \gamma + g(t) \right] \right\} + \frac{H}{h} \sqrt{gh} A'_{22} u \sin \gamma \cdot \\
 & \left\{ \text{sech}^2 \epsilon \left[\ell \cos \gamma - g(t) \right] - \text{sech}^2 \epsilon \left[\ell \cos \gamma + g(t) \right] \right\} \quad (148)
 \end{aligned}$$

$$\begin{aligned}
 N_{(\text{waves})} = & - \frac{H}{h} \sqrt{gh} c \tan \gamma (\rho B d + A'_{22}) \cdot \left\{ \ell \operatorname{sech}^2 \epsilon \left[\ell \cos \gamma - g(t) \right] \right. \\
 & + \ell \operatorname{sech}^2 \epsilon \left[\ell \cos \gamma + g(t) \right] \\
 & - \frac{1}{\epsilon \cos \gamma} \tanh \epsilon \left[\ell \cos \gamma - g(t) \right] \\
 & \left. - \frac{1}{\epsilon \cos \gamma} \tanh \epsilon \left[\ell \cos \gamma + g(t) \right] \right\} \\
 & + \frac{H}{h} \sqrt{gh} A'_{22} \ell u \sin \gamma \left\{ \operatorname{sech}^2 \epsilon \left[\ell \cos \gamma - g(t) \right] \right. \\
 & \left. + \operatorname{sech}^2 \epsilon \left[\ell \cos \gamma + g(t) \right] \right\} \tag{149}
 \end{aligned}$$

$$\begin{aligned}
 K_{(\text{waves})} = & \rho g H \epsilon \tan \gamma |GM| B d \left\{ \operatorname{sech}^2 \epsilon \left[\ell \cos \gamma - g(t) \right] \right. \\
 & \left. - \operatorname{sech}^2 \epsilon \left[\ell \cos \gamma + g(t) \right] \right\} \tag{150}
 \end{aligned}$$

Since the solitary wave action occurs near shore, where the boat will generally be controlled to keep the angle γ small, the approximations $\cos \gamma \approx 1$, $\sin \gamma \approx \tan \gamma \approx \gamma$ can be made to simplify the foregoing expressions. When applying these results to the head sea retraction operation, the solitary wave form is changed to

$$\eta = H \operatorname{sech}^2 \left\{ \sqrt{\frac{3H}{4h^3}} \left[x \cos \gamma + ct + \cos \gamma \int u dt \right] \right\}, \tag{151}$$

the sign of u is changed in the arguments of hyperbolic functions, and the signs of $Z_{(\text{waves})}$ and $N_{(\text{waves})}$ are also changed, just as in the case of the treatment of oscillatory waves discussed previously.

The forces and moments due to a solitary wave decrease rapidly for large values of time, and hence they are similar in form to transient impulse effects. This behavior is appropriate to the treatment of breaker effects physically, and the short time of action allows simple solution of the motion responses. The only problem associated with the treatment of these forces is the continuous variation that must be computed for the parameters

such as H , h , etc. as the ship moves, and the relation of the wave geometry to the ship location at every instant. Similarly it is necessary to represent some type of "transition" of the wave forces as the wave field changes from oscillatory to solitary wave form, and this requires maintaining a continuity in time of the various forces acting on the boat during the transition period. These same requirements and problems exist for the case of following seas when approaching the beach, and also head seas for retraction, with the time and space reference relations for boat and wave field as primary considerations. A discussion of computational techniques for generating the solitary wave field and the forces associated with it is given in a later section of this report.

The forces due to the run-up water elevation following breaking are approximated as equivalent to those associated with a sudden elevation of the craft to a new height, together with a force in the x -direction, a force in the y -direction, and a yawing moment. The longitudinal velocity field in the run-up bore produces a net flow relative to the craft, given by $(u_R \pm u)$, which is interpreted as an equivalent current, where u_R is defined in Equation (33). The axial force produced by this flow is considered to be equivalent to a resistance force, which is assumed to be frictional, and which can act to propel the ship forward in a following sea, as long as the ship is in the flow field, and it adds additional resistance in a head sea situation. The method of synchronizing the run-up flow with the solitary waves, and for evaluating forces, is presented in a later section of the report.

The longitudinal force is represented by

$$X_R = \frac{\rho}{2} C_f S (u_R - u)^2 \cos \gamma \quad (152)$$

for the following sea case, where C_f is the friction coefficient and S the underwater wetted surface area, and by

$$X_R = - \frac{\rho}{2} C_f S (u_R + u)^2 \cos \gamma \quad (153)$$

in the head sea case. When the craft is beached and has no forward speed, the same expression as Equation (147), with $u = 0$, is valid and represents a force that occurs at the same periodicity as the run-up flow field. The use of these expressions neglects any short term impulse-like action due to the initial contact of this flow field with the craft hull, and is an approximation in that sense.

The transverse force in the run-up field is assumed to be the same as that due to a current acting on the craft. On the basis of analysis of deep water model tests as presented in [25], this lateral force is given by

$$Y_R = .6 Ld (u_R \pm u)^2 \sin \gamma \quad (154)$$

where the + sign is for head seas and the - sign for following seas. The appropriate value of d for each configuration, and the value of γ for the particular case of either head or following seas (as evaluated during the simulation) determines the value of the lateral force in this case. The results are also valid for the situation where the craft is beached, with $u = 0$. The yawing moment, also found from [25], is represented by

$$N_R = .035 L^2 d (u_R \pm u)^2 \sin 2\gamma \quad (155)$$

with the same interpretation of signs, parameter values, etc. as for the lateral force. In all of the preceding expressions it is necessary to relate the run-up flow field to the craft geometrically, since no force will act on the craft until both craft and run-up flow are in coincidence and the flow field acts upon the craft. Further discussion of this requirement will be presented in a later section.

The vertical force and pitch moment due to the run-up is approximated by the hydrostatic effect alone, as indicated e.g. by Equation (112), with special mathematical functions representing the run-up as a function of time and space. With the run-up R assumed to have a constant magnitude for a given offshore sea condition, and the constant ship beam, the vertical force and pitch moment are given by

$$Z_R = -\rho gBR \int_{\text{hull}} f_R(\xi, t) d\xi \quad (156)$$

and

$$M_R = \rho gBR \int_{\text{hull}} \xi f_R(\xi, t) d\xi \quad (157)$$

where $f_R(\xi, t)$ is a special function describing the time and space dependence of the run-up (a detailed treatment of this function is given in a later section). Since the run-up occurs in the close inshore region near the beach, the wave angle β tends toward a small angle, so that dependence of the vertical force and pitch moment in terms of the parameter $\cos \gamma$ can be neglected.

11. WIND EFFECTS

Forces and moments due to wind acting on the above-water portions of the hull act on the boat in the horizontal plane. Limited data on wind forces exists for particular ships, but no direct information is available for the present assault boat.

In order to estimate these effects, it is necessary to determine the relative wind speed and direction with respect to the ship in its own reference frame. Following the procedure in [26], with the wind speed U_W and direction ψ_W referred to the inertial reference frame as shown in Figure 9, the relative wind speed components along the ship axes are

$$u_{RW} = U_W \cos (\psi_W - \psi) - u \quad (158)$$

$$v_{RW} = U_W \sin (\psi_W - \psi) - v \quad (159)$$

The resultant wind is then given by

$$U_{RW} = \sqrt{u_{RW}^2 + v_{RW}^2} \quad (160)$$

at the angle of attack

$$\mu = \tan^{-1} \left(- \frac{v_{RW}}{u_{RW}} \right) \quad (161)$$

relative to the u axis, as shown in Figure 9. The angle μ is further defined by

$$\begin{array}{ll} 0^\circ < \mu < 90^\circ & ; \quad u_{RW} < 0 \quad , \quad v_{RW} > 0 \\ 90^\circ < \mu < 180^\circ & ; \quad u_{RW} < 0 \quad \quad v_{RW} > 0 \\ 180^\circ < \mu < 270^\circ & ; \quad u_{RW} > 0 \quad \quad v_{RW} < 0 \\ 270^\circ < \mu < 360^\circ & ; \quad u_{RW} > 0 \quad \quad v_{RW} < 0 \end{array} \quad (162)$$

The above relations are valid when the wind angle ψ_W and the ship yaw orientation ψ are measured with respect to the inertial reference in Figure 6 for the following sea condition. They are also valid when measured relative to the same reference for determining the angle ψ for the case where the boat is heading away from shore, as indicated in Figure 6, due to the change in ship axes.

The wind force in the direction of the resultant wind velocity U_{RW} is given in [27] as

$$D_W = \frac{\rho_a}{2} C_D A_{proj} U_{RW}^2 \quad (163)$$

where ρ_a is air density, C_D is an average drag coefficient, and A_{proj} is the silhouette area of the above-water portion of the boat projected on a vertical plane normal to the direction of the relative wind U_{RW} . The quantity D_W in Equation (163) is computed,

and assuming a small lift force generated by the boat, the components of D_w are resolved along the boat x- and y-axes. With A_1 the effective frontal above-water area of the boat hull side, and A_2 for the lateral above-water area, the resulting forces are given by

$$X_{(wind)} = -\frac{\rho_a}{2} C_D (A_1 |\cos \mu| + A_2 |\sin \mu|) U_{RW}^2 \cos \mu \quad (164)$$

and

$$Y_{(wind)} = \frac{\rho_a}{2} C_D (A_1 |\cos \mu| + A_2 |\sin \mu|) U_{RW}^2 \sin \mu \quad (165)$$

Since the boat hull is almost symmetrical fore and aft, for the approximation used in the present study, the above-water portion may also be viewed in that way, except for the influence of the large bow ramp and the pilot house.

The moment due to the wind depends on the location of the (effective) center of projected area, and as an estimate this is represented by

$$N_{(wind)} = 0.3 L \cdot \frac{\rho_a}{2} C_D (A_1 |\cos \mu| + A_2 |\sin \mu|) U_{RW}^2 \cdot (1 - |\sin \mu|) \text{sign}(\sin \mu) \quad (166)$$

The value of 0.3 represents the limit (as a fraction of ship length) of the wind pressure centroid as the wind heading changes, and this is consistent with the calculations for different vessels presented in [25].

An evaluation of the numerical parameters appropriate to the LCM (6) hull in its two operating modes is presented in [2].

12. BEACH FORCES

When the craft lands on the beach, i.e. reaches a point where the bow portion of the keel touches the bottom, it is assumed that all forward motion stops and the beached condition is achieved with $u = 0$. In that case forces due to the waves in the form of run-up will continue to act on the craft, especially in the lateral plane, where the yawing moment especially requires attention on the part of the coxswain to provide control in order to maintain the craft heading normal to the beach. Due to the lack of knowledge of precise soil properties, the extent of penetration into the beach, etc. it is almost impossible to determine the forces acting on the craft to "hold" it on the beach due to the interaction between the beach soil material and the craft.

In order to represent some action of the beach, the most significant reactive force considered is that in the axial

direction, i.e. the force that must be overcome by the ship propellers in order to "free" it from the beach. When this longitudinal force is overcome the craft can move out into deeper water to encounter the various hydrodynamic excitation forces and respond to them. The restraining longitudinal force is assumed to be equal to the value of the thrust of both propellers, for a particular value of propeller rotational speed which is selected as that considered representative for moving a landing craft off a beach, according to operational experience or other guiding dictates of the simulator training officer. Using the expression for the thrust of the propellers in the retraction mode, the beach force in the longitudinal direction is

$$X_{\text{(beach)}} = - 0.95 n_t^3 \quad (167)$$

where the value of n_t is selected for a particular training mission. This same force expression can also be applied when the craft is encountering the beach during landing in order to assist in bringing it to a final stop.

For the lateral force an arbitrary threshold resisting value can be selected so that the run-up lateral force does not cause any significant sideward motion. The yawing action must be corrected by coxswain control via differential propeller thrust, and hence no yawing moment due to the beach is considered. Due to small roll motions anticipated in this case on the beach, just as in the case of run-up effects directly, that quantity is also neglected. Since the vertical force and pitching moment are due to hydrostatic effects of the run-up, as shown in Equations (156) and (157), no additional beach forces on these modes are considered, since the resulting motions are only in response to the run-up flow, which occurs in a time-varying periodic manner (see discussion in a later section).

B. COMPUTATIONAL CONSIDERATIONS

The equations developed in the preceding analysis are to be applied to a simulator that represents the actual motions of the craft in real time. Solutions for the equations must be obtained with a computer that would also be able to represent the wave field characteristics in proximity to the boat, as well as the motions of the craft that occur simultaneously due to the wave-induced excitation and the coxswain-commanded control actions. The equations themselves are developed in a mathematical form, but the implementation on a computer is a separate and distinct task. Examination of the various elements entering into the entire mathematical model of the craft motion, as well as the environmental wave field, indicates a preference for a particular type of computer for representing each element in the overall simulation.

The wave generation procedure on the computer is best carried out by means of a digital computer, since the modifications necessary to account for the influence of varying depth as a function of time as the craft progresses along the beach, and the transition to the solitary wave form, are most easily carried out using that type of computer. The logical decisions; the iterative routine to compute wave number; and the means of computation of the different mathematical functions essential for the representation of a wave system are most suitable to a digital computer, and hence that is the recommended procedure to be used. Since the wave excitation forces are made up of functions involving wave parameters, as well as similar mathematical functions, the wave-induced forces and moments should also be computed using a digital computer technique. The computer operations for the entire simulation assume the existence of information in an analog domain, which is converted into the digital domain by use of A-D converters, so that the digital computation can proceed. The output of the digital program is then sent through D-A converters so that this data is then in the proper form for direct application in the analog representations of the dynamic equations of motion.

A summary of the final equations of motion, together with functional block diagrams and associated explanatory discussion, is presented in the Appendix of this report. This Appendix also contains the flow charts for computation of wave characteristics, time history forms, etc. as well as the means of computing the associated wave forces. The computational technique described above is directed toward use of both analog and digital computers, together with a hybrid interface. The use of a hybrid computer system as a means of carrying out the required equation solutions, etc. is not proposed as the only possible means of implementing the present mathematical model. However it is the type of system present at Oceanics, and it can provide real time solutions of the dynamic equations of motion via the analog portion of the system. Assuming that a general purpose digital computer with proper capacity were available, the basic technique of solution indicated

in the flow diagrams could also be implemented on that type of machine. Questions concerning the integration method, stability considerations, sampling times, etc. that would affect the feasibility of carrying out such computations in real time are considered in a limited fashion in a later portion of this section.

When carrying out the wave field computations, the concept proposed is to be able to evaluate a wave elevation, velocity, etc. at any point on the free surface, as a function of time, independent of the location of the craft. Particular locations at the craft, as it progresses on toward the beach or as it retracts, can then be considered as a means of relating the environment and the craft behavior. This point of view also allows evaluation of the various wave forces, by referring them to the wave as measured at the CG of the craft. Similarly it allows the separate computation of oscillatory waves, solitary waves, and run-up elevation, each in the appropriate region for their occurrence.

The spatial and time-varying properties of the oscillatory wave and the corresponding wave forces and moments are properly simulated as shown in previous sections by introducing the function $f(t)$ (defined in Equations (123) and (132)) referenced to a fixed point offshore. The situation is different with respect to solitary wave expressions since they, by their hyperbolic nature, represent only a single wave. A wave train, however, can be generated in a simple fashion by a reinterpretation of the argument $g(t)$ (defined in Equation (140)) within the hyperbolic functions. The period of shoaling breaker waves is approximated to be the period of maximum energy of the offshore wave spectrum, T . The crest to crest distances is then simply cT where c (the wave propagation speed) varies according to distance offshore. A train of solitary waves can then be generated if the argument $g(t)$ repeatedly passes through zero with periodicity cT . The most convenient manner of implementing this in a digital computer is through the use of a mod function. A mod function, $\text{mod}(x,y)$ is defined as $x - [x/y]y$ where $[x]$ is an integer with magnitude of not more than x and sign the same as x . It is easily seen that the proper function is

$$m(t) = \text{mod} \left(g(t), cT \right) - \frac{cT}{2} \quad (168)$$

which when introduced into the solitary equations for wave elevation, forces, and moments will give the correct spatial and time-varying properties.

The point of transition between oscillatory waves and solitary waves as previously discussed is known once the offshore wave spectrum and beach slope is selected. A smooth transition is desirable for many reasons, but particularly with respect to forces and moments so that unwarranted transients are not introduced in the craft motions. A smooth transition from one region to the other can be most easily accomplished if a transition zone is specified in which the wave property of interest from the region the craft is leaving is decayed out while the similar

property of the region in which the craft is entering is smoothly introduced. The width of the transition zone is chosen to be about a boat length. Thus the wave elevation in the transition zone, upon leaving the oscillatory region, could be represented by

$$\eta(\text{total}) = \frac{(L-s_z)}{L} \eta(\text{osc.}) + \frac{s_z}{L} \eta(\text{sol.}) \quad (169)$$

where s_z is the distance traversed through the transition zone, where the transition zone extends from locations of length $\frac{L}{2}$ ahead and behind the transition point (defined by relations in Equation (25)). With the solitary wave height taken equal to the significant height of the offshore waves, at the transition point, the height grows as the wave propagates into shallower water in accordance with Greens's law, Equation (27). Breaking occurs when the wave height and the local water depth satisfy Equation (26), and this point can be established by initial computations when the transition point, offshore significant height, and beach slope are given or established (in the case of the transition point, in terms of the other parameters specified).

Another problem in the simulation is to synchronize the run-up with the solitary waves at breaking. Since the point of breaking is known beforehand, through the use of the mod function the times at which the solitary wave crests arrive at the breaker line is known. These are the times at which the run-up function is initiated.

The run-up flow field is established following breaking, and it is assumed to have a time extent of $\frac{T}{2}$, with T the period of maximum spectral energy offshore. This is followed by a time interval of $\frac{T}{2}$ in which no elevation occurs, and then the system repeats over and over again as a time history, similar to a series of square waves. This idealized model is assumed to have a propagation speed c_R defined by Equation (32), and the spatial and temporal variation is expressed in terms of the function

$$s = x_R - c_R t \quad (170)$$

where x_R is the longitudinal distance measured from the breaking point, along the x_o -axis, and the time t in Equation (170) is measured from the instant of wave breaking in each case. To relate this result to other parameters developed in the analysis, the relation

$$x_R = (x_o - x_{o_b}) + \xi \quad (171)$$

is defined, where x_{o_b} is the inertial frame coordinate (along

x_0 -axis) at which breaking occurs, x_0 is the reference position of the ship CG (or any space points at which the run-up form is desired to be determined), and ξ is the "dummy" variable along the ship hull (measured from the origin at the CG) that allows determination of the relative position of the run-up elevation. The run-up is then functionally represented by the expression

$$R(x_0, t) = R \cdot 1 \left[\frac{c_R T}{2} - \text{mod}(s, c_R T) \right] \\ = R f_R(\xi, t) \quad (172)$$

with $1 \left[\right]$ the unit step function, where the function $f_R(\xi, t)$ in Equations (156) and (157) is then defined.

Another remaining consideration is the question of sampling rate in real time at which the wave forces and moments have to be evaluated and inputted to the dynamic system implemented on the analog portion of the computers. The sampling theorem requires (see e.g. [28]) the sampling rate to be at least twice the highest frequency of interest present in the dynamics to avoid aliasing. Since the bandwidth is about 2.5 times the natural frequency, for this craft the sampling rate should be at least 5 times the highest natural frequency. This sampling rate should be considered to be only a lower bound and a higher sampling rate, perhaps 10 or more times the highest natural frequency is more desirable.

If the overall simulation is to be carried out in real time by means of a digital computer, it is necessary to choose an appropriate integration scheme for that purpose, with the various requirements of the wave field, forces, etc. computations coordinated consistently within the solution technique. A required criterion of a suitable integration technique is efficiency, i.e. that it accomplish the required integration in a minimum of time so that real time simulation be accomplished. Another requirement is accuracy, but accuracy is often indirectly related to efficiency since a reduction in the integration interval often produces a concurrent increase in accuracy. A third criterion is stability, where the integration method does not permit any accumulated errors to grow or oscillate without bound over the length of time of particular simulation applications. All of these factors are related, in very intricate ways, and there is no single guidance to indicate a choice of any single method for the present problem (or for that matter, for any arbitrary real-time vehicle simulation). However, while there are many integration schemes to choose from, for a general systems simulation where speed and accuracy is of paramount importance and numerical stability is assured, the Runge-Kutta-Merson method [29] is recommended on the basis of a comparative study of the performance of this method with the other common methods [30].

SECTION IV

CONCLUSIONS

The six degree of freedom mathematical model for an assault boat developed herein is concluded, on the basis of the experiments presented in [2], to be an accurate representation of the boat motions from both the hydrostatic and hydrodynamic effects of body-fluid interaction in the presence of waves. The waves are considered to have been generated by an offshore random sea and are progressing towards the shoreline. Account is taken of the change in wave character and direction resulting from the influence of a sloping beach to the time of breaking, which is followed by run-up onto the beach. Effects of run-up and other causes of boat motion, namely, propulsion and wind effects and the coxswain control commands are detailed.

It is concluded that this model, together with the computational techniques discussed herein, serves as an adequate basis for the development of a real time simulator for the purposes of coxswain training.

SECTION V

REFERENCES

1. Blee, M., "Model Tests to Evaluate the Performance of a Twin Screw Landing Craft for Oceanics, Inc.," Report No. X/O/1137, Feb. 1969, British Hovercraft Corp., Ltd., England.
2. Kapan, Paul; Ward, Lawrence W.; and Chung, Yong K., "Final Report on Development of a Mathematical Model Representing Assault Boat Motion in Waves," Report No. 69-66, July 1969, Oceanics, Inc., Plainview, New York.
3. Korvin-Kroukovsky, B. V., Theory of Seakeeping, New York, Soc. of Naval Arch. and Marine Eng., 1961.
4. Kaplan, Paul and Sargent, Theodore P., "Theoretical Study of the Motions of an Aircraft Carrier at Sea," Report No. 65-22, Jan. 1965, Oceanics, Inc., Plainview, New York.
5. "Landing Craft and Their Employment," Issued by Commander, Amphibious Training Command, U. S. Pacific Fleet, Jan. 1965.
6. "56' Landing Craft, Mechanized Mark 6, Mod 2 (LCM 6) FY 67," Booklet of Plans supplied by Naval Ship Systems Command.
7. Kinsman, Blair, Wind Waves, Englewood Cliffs, New Jersey, Prentice Hall, Inc., 1965, Chapters 3 and 5.
8. Davis, M. C. and Zarnick, Ernest E., "Testing Ship Models in Transient Waves," Proc. Fifth Symp. on Naval Hydrodynamics, Bergen, Norway, Sept. 1964, Office of Naval Research, Wash., D. C.
9. Kaplan, Paul, "A Study of Prediction Techniques for Aircraft Carrier Motions at Sea," Jour. of Hydronautics, Vol. 3, No. 3, July 1969.
10. St. Denis, M. and Pierson, W. J. Jr., "On the Motions of Ships in Confused Seas," Trans. Soc. of Naval Arch. and Marine Eng., 1953, New York.
11. Wiegel, Robert L., Oceanographical Engineering, Englewood Cliffs, New Jersey, Prentice Hall, Inc., 1964, Chapters 3 and 7.
12. Stoker, J. J., Water Waves, New York, Interscience Publishers, Inc., 1957.
13. Biesel, F., "Study of Wave Propagation in Water of Gradually Varying Depth," Gravity Waves, U. S. Natl. Bur. of Stand. Circular 521, pp. 243-253.

14. Wiegel, Robert L., *op.cit.*, Fig. 17.9, p. 452.
15. Divoky, David; Le Méhauté, Bernard; and Lin, Albert, "Breaking Waves of Gentle Slopes," Tetra Tech., Inc., Pasadena, Calif. (To be published in Jour. of Geophysical Research.)
16. "Nomenclature for Treating the Motion of a Submerged Body Through a Fluid," Tech. and Res. Bulletin No. 1-5, April 1950, Soc. of Naval Arch. and Marine Eng., New York.
17. Lamb, Horace, Hydrodynamics, New York, Dover Publications, 1932, Chapt. VI.
18. Kaplan, Paul, "Application of Slender Body Theory to the Forces Acting on Submerged Bodies and Surface Ships in Regular Waves," Jour. of Ship Research, Nov. 1957.
19. Grim, O., "Die Schwingungen von schwimmenden, zweidimensionalen Körpern," Report No. 1171, Sept. 1959, Hamburgische Schiffbau-Versuchsanstalt, Germany.
20. Patterson, W. Robert, "The Stability of the Amphibious Craft LVTP-X12 in Waves and Surf," Report No. 68-1, Jan. 1968, Mass. Inst. of Tech., Dept. of Naval Arch. and Marine Eng., Mass.
21. Telephone communication with Marinette Marine Corp., Marinette, Wisc. (LCM (6) manufacturer.)
22. Norrbin, Nils H., "A Study of Course Keeping and Manoeuvring Performance," Publication No. 45, 1960, Swedish State Shipbldg. Exptl. Tank, Sweden. Also available in Proc. First Symp. on Ship Maneuver., David Taylor Model Basin Rpt. No. 1461, Oct. 1960.
23. Gerritsma, J.; Van Den Bosch, J. J.; and Beukelman, W., "Propulsion in Regular and Irregular Waves," International Shipbldg. Progress, Vol. 8, No. 82, June 1961.
24. Fuchs, R. A. and MacCamy, R. C., "The Oscillations of Ships in a Solitary Wave," Proc. of First Conference on Ships and Waves, Hoboken, New Jersey, Oct. 1954.
25. Hawkins, S.; Taggart, R.; and Hoyt, E. D., "The Use of Maneuvering Propulsion Devices on Merchant Ships," Report No. RT-8518, Jan. 1965, Robert Taggart, Inc., Maryland.
26. Uram, E. M.; Crane, C. L.; and Chey, Y. H., "Equations of Motion for Mooring and Docking Maneuvers of a Destroyer and a Surfaced Submarine," Tech. Rpt. NAVTRADEVCON 1423-1, Nov. 1966, Naval Training Device Center, Florida.

27. Saunders, H. E., Hydrodynamics and Ship Design, Vol. I and II, New York, Soc. of Naval Arch. and Marine Eng., 1957.
28. Hamming, R. W., Numerical Methods for Scientists and Engineers, New York, McGraw-Hill Book Co., 1962.
29. Lance, G. N., Numerical Methods for High Speed Computers, London, Iliffe & Sons, 1960.
30. Martens, H. R., "A Comparative Study of Digital Integration Methods," Simulation, Vol. 12, No. 2, Feb. 1969.

TABLE 1

NUMERICAL VALUES OF LCM (6) SHIP CHARACTERISTICS

	<u>Heavy</u>	<u>Light</u>
Length, ft.	54	51
Beam, ft.	14	14
Draft, ft.	3.25	2
Displacement, tons	58	28
LCG, ft. forward of midships	1.32	1.32
Vertical CG height, above keel, ft.	4.33	3.4
Pitch gyradius/LBP	.24	.24
Yaw gyradius/LBP	.26	.26
Heave period,* sec.	2.9	-
Pitch period,* sec.	3.1	-
Roll period,* sec.	3.4	-

*Obtained from calm water free oscillation model tests at heavy load condition, zero speed.

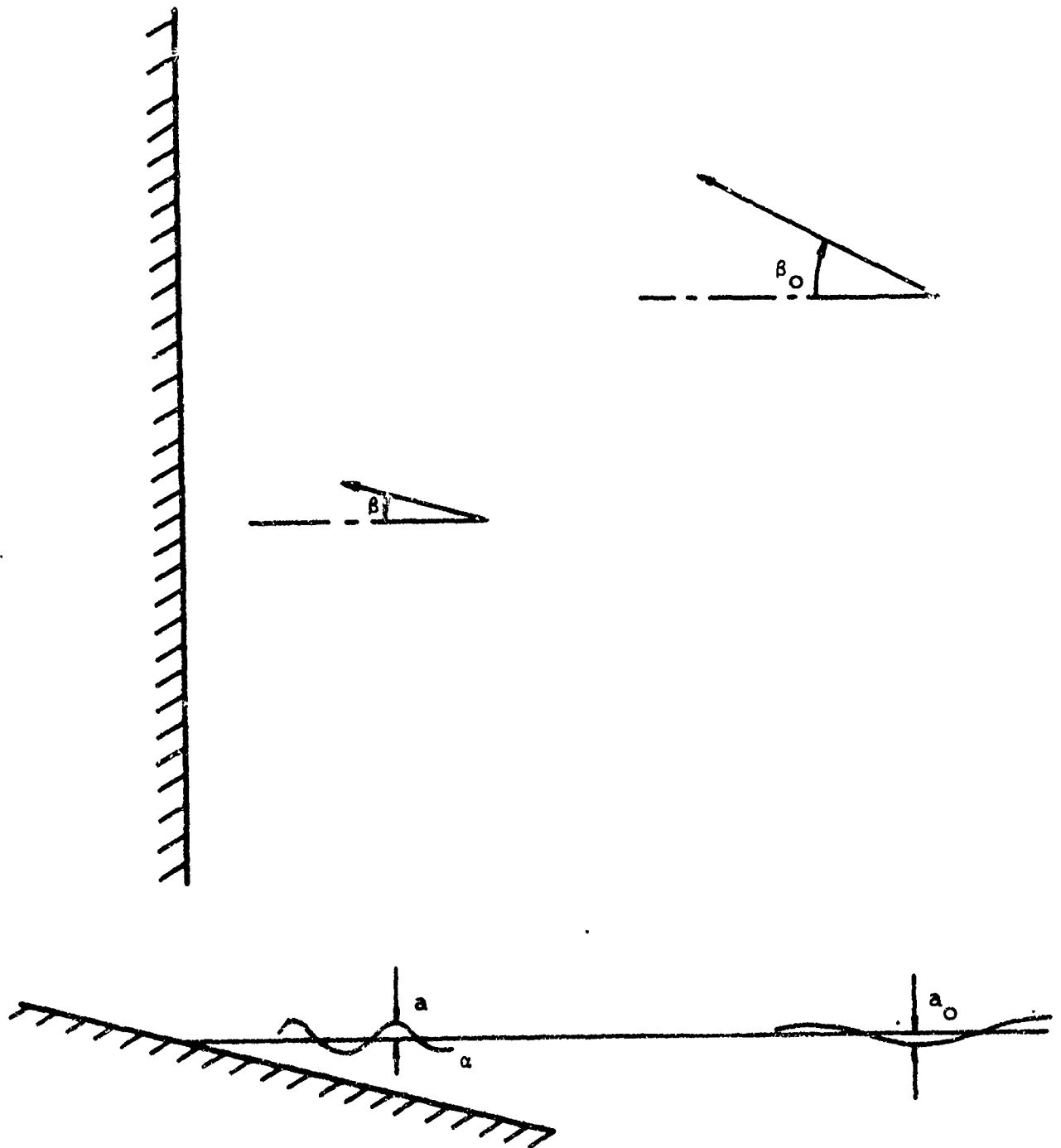


Figure 1. Wave propagation toward shore along sloping beach

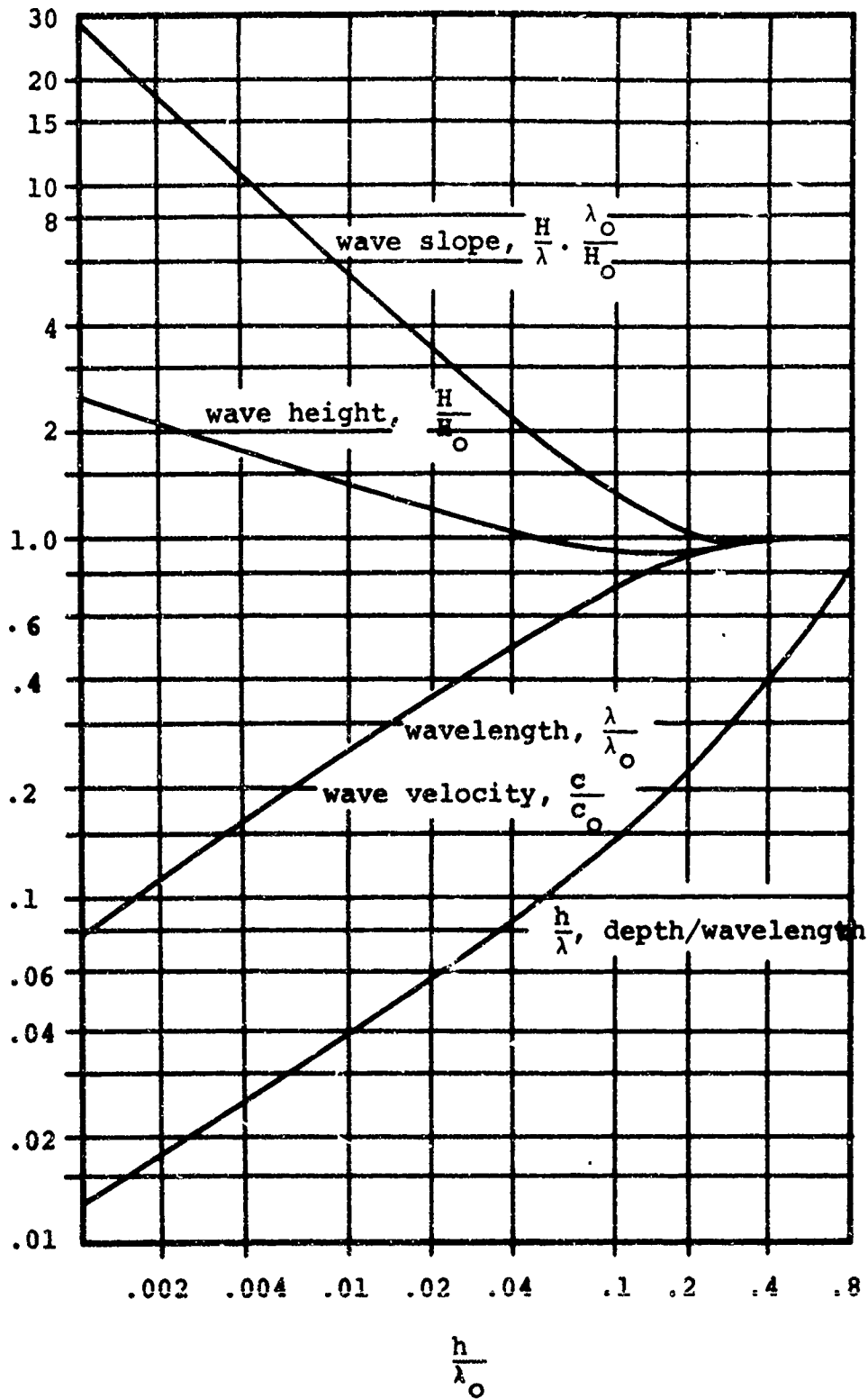


Figure 2. Variation of wave characteristics, relative to deep water values, as function of ratio of depth to deep water wavelength

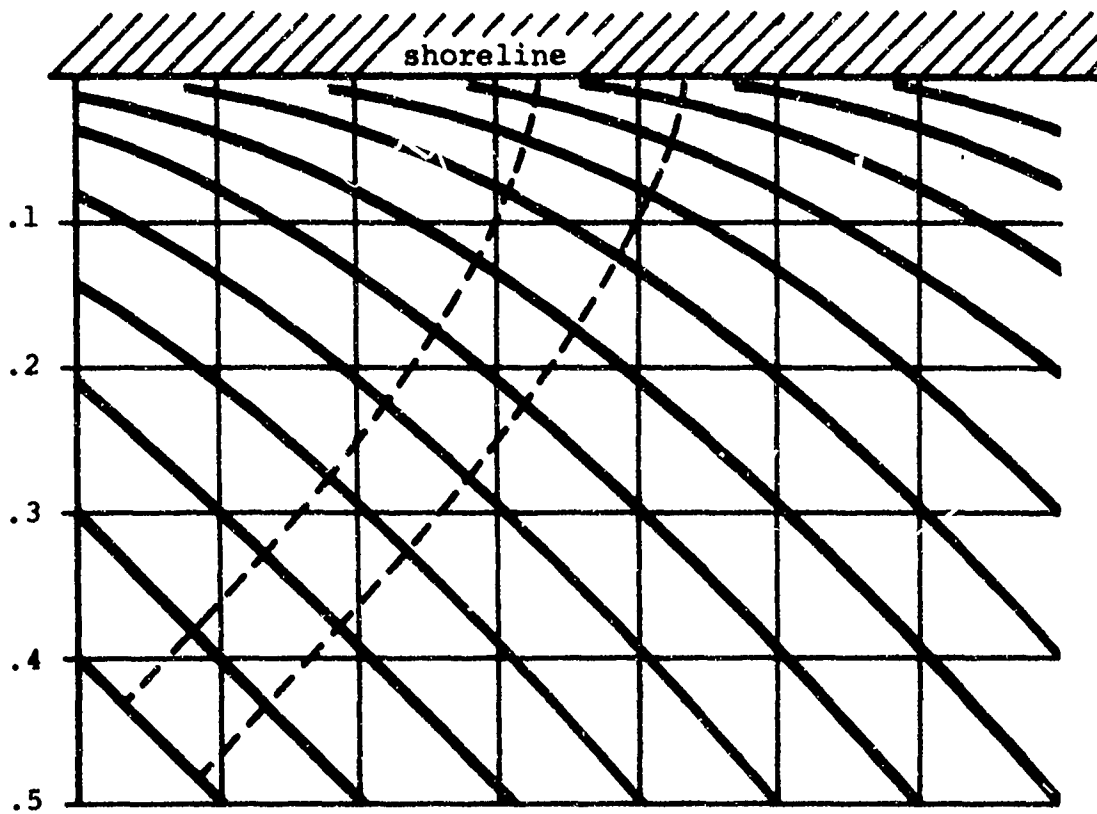


Figure 3. Wave refraction diagram for waves approaching a uniformly sloping beach, $\beta_0 = 45^\circ$

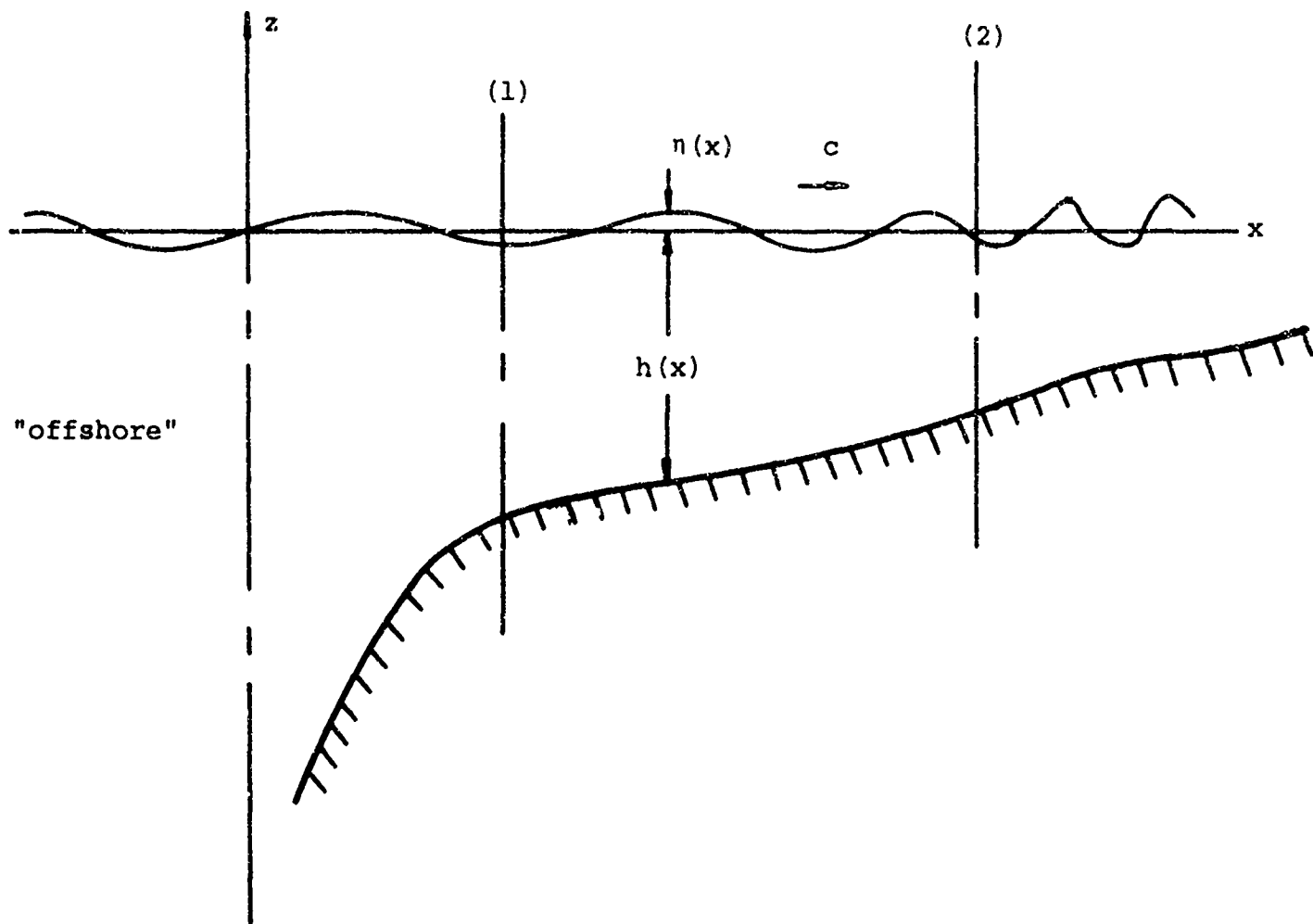


Figure 4. Waves approaching beach over varying bottom contour, with spatial reference point locations

$V_w = 19$ kts.
 Area = 5.964 ft.²

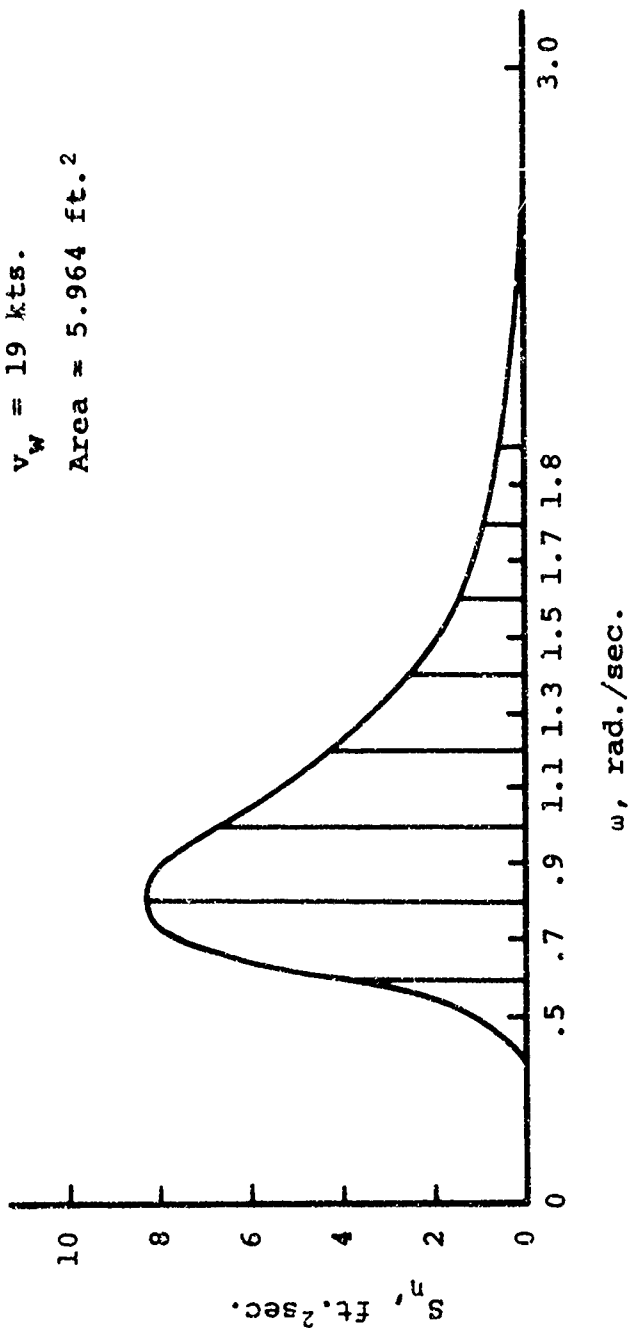


Figure 5. Sea State 4 Wave Spectrum Decomposition

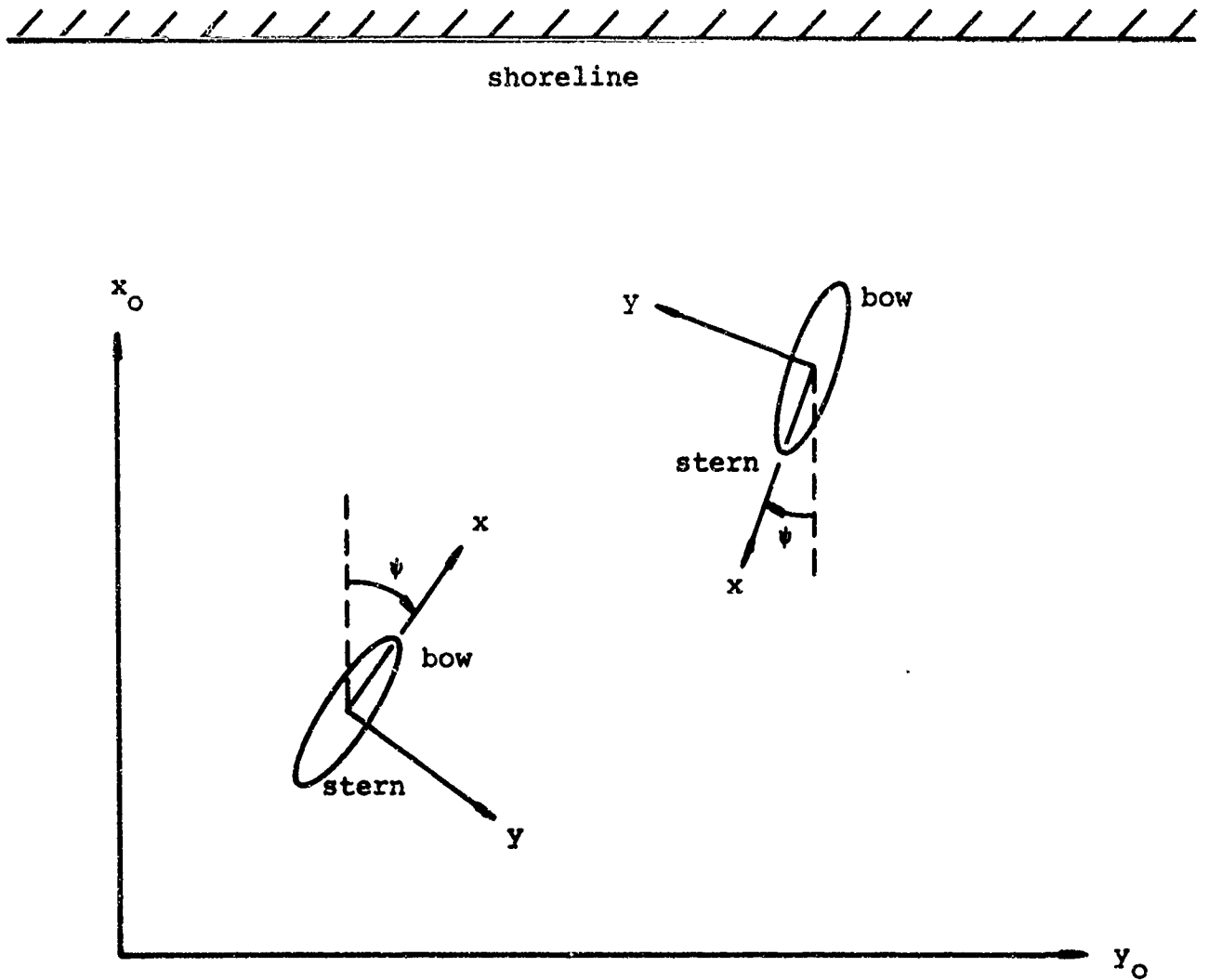


Figure 6. Relation of ship axes, shore position, and inertial reference frame

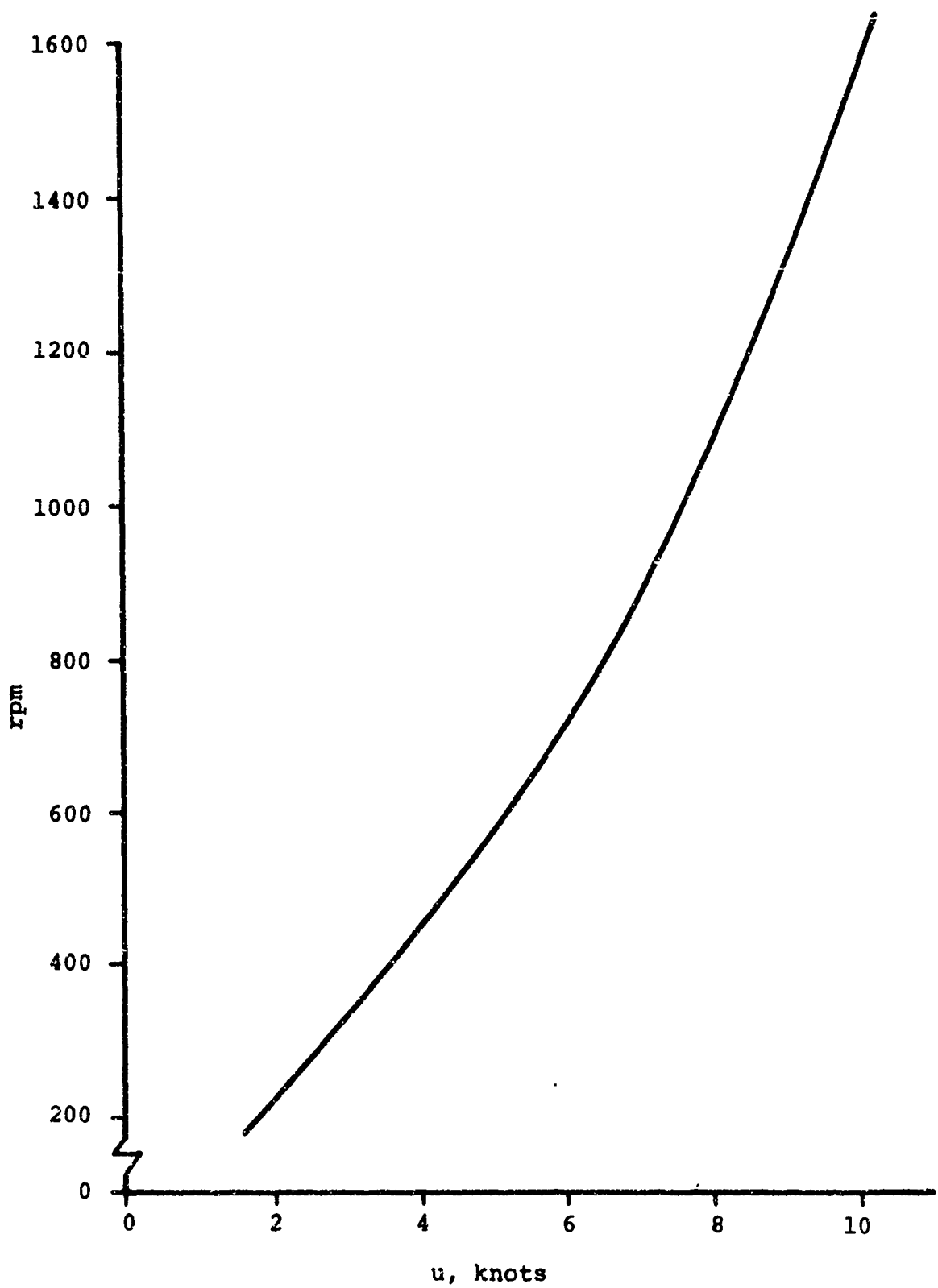


Figure 7. Variation of propeller rpm with speed at self-propulsion, twin-screws, ahead motion, heavy displacement

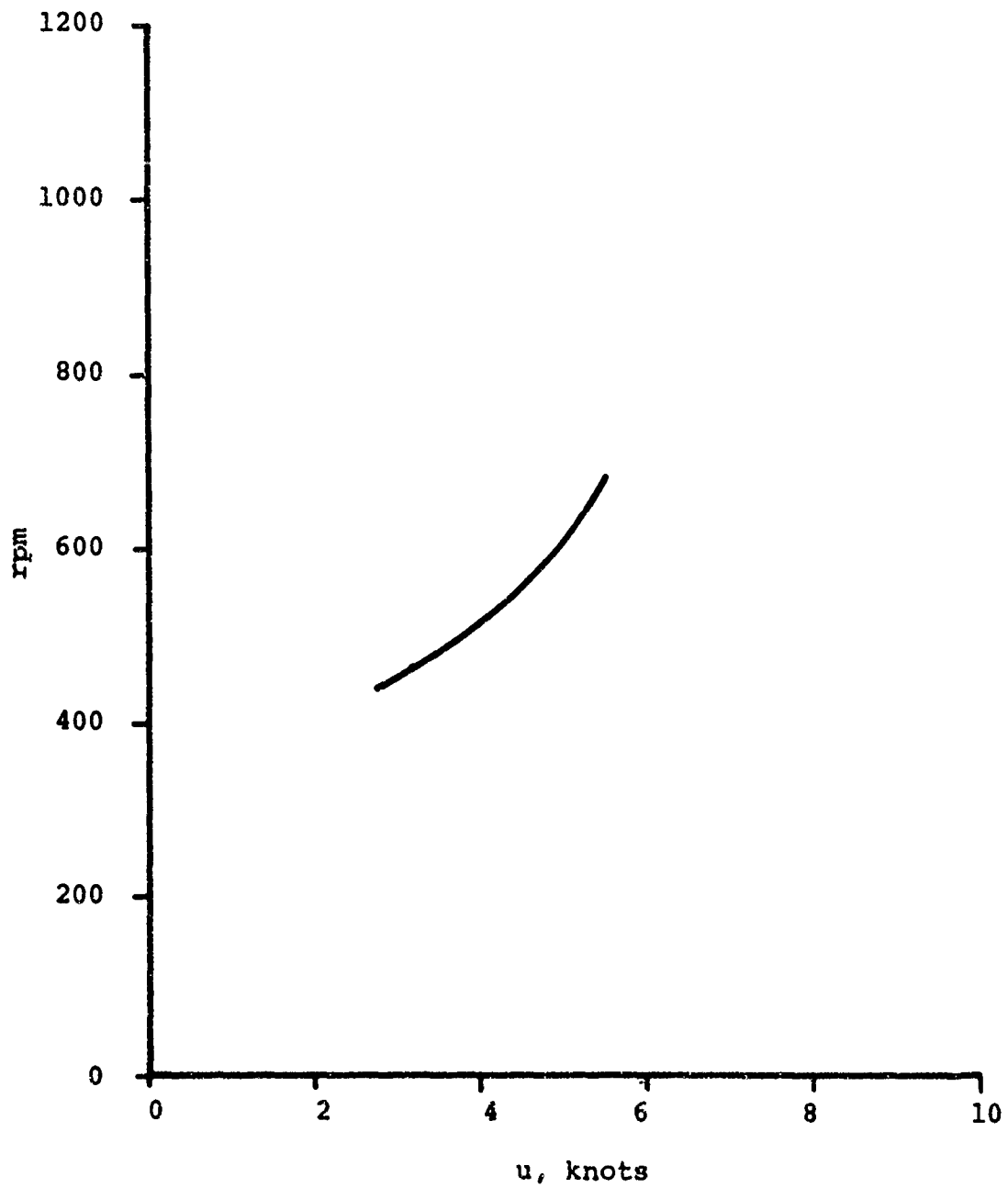


Figure 8. Variation of propeller rpm with speed at self-propulsion, twin-screws, astern motion, light displacement

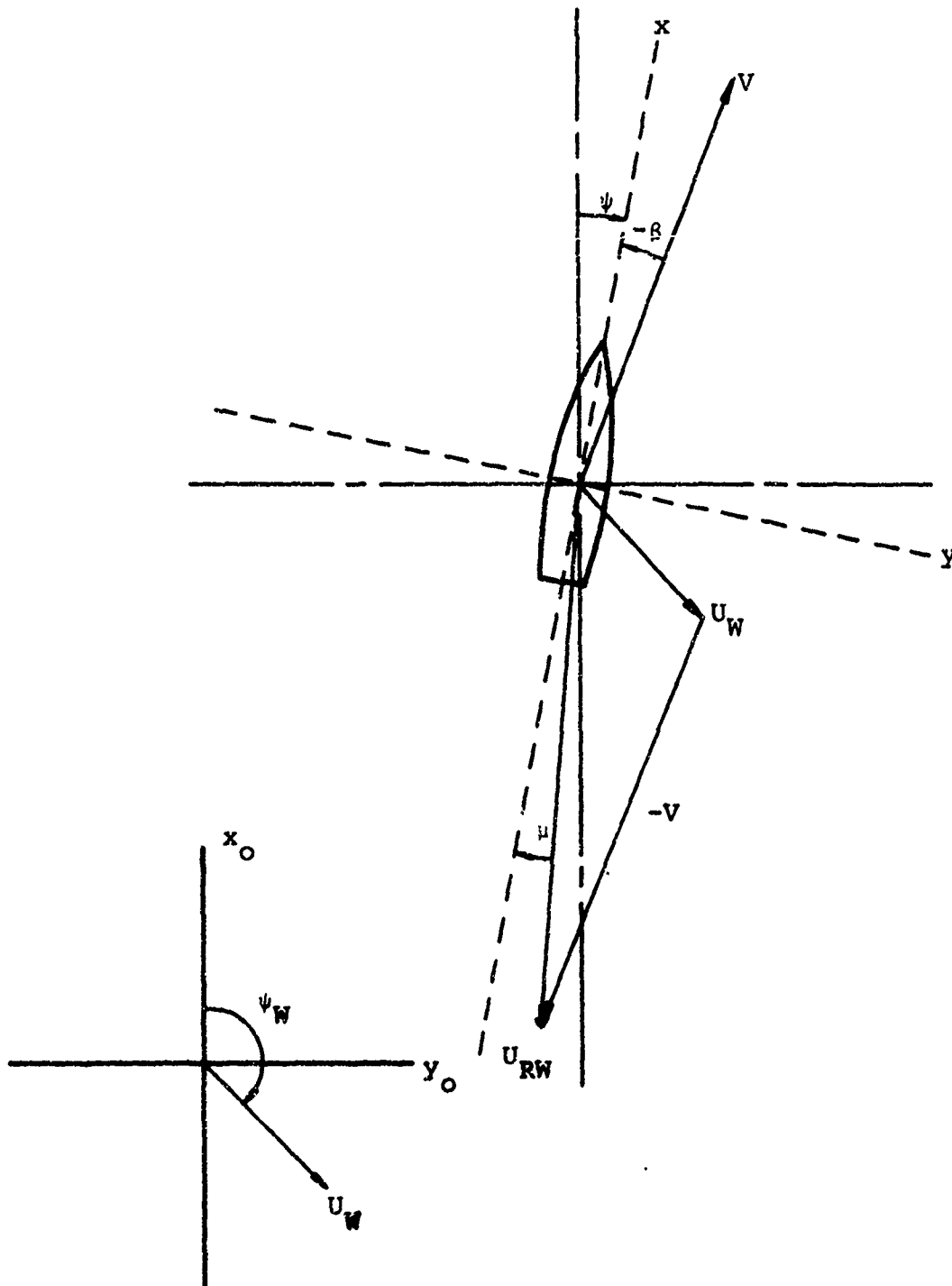


Figure 9. Relation of resultant wind velocity to ship axes

APPENDIX A

EQUATION SUMMARY AND SOLUTION PROCEDURES

The final equations of motion are represented below, in general form and/or with reference to other expressions within this report, for operating conditions corresponding to approaching (heavy configuration) or retracting (light configuration) from a sloping beach through waves. The neglect of coupling between planes of motion, the reference to axes appropriate to seakeeping analyses, and other simplifications reduce or delete various nonlinear effects, thereby allowing ease of computational requirements for solution of the equations. The compiled equations are presented for each degree of freedom, with a separate discussion following the presentation to indicate the various procedures (in flow chart form) for computing the wave properties, forces, etc. together with their use in the equations. The procedures for solution of the equations are also outlined in a flow diagram, and reference is given to particular equations in the main text where various parameters, operations, etc. are defined and/or derived. Amplifying discussion is given, where required, to explain some of the procedures in the computations. The numerical values appropriate to various parameters in the equations are given in [2] or are pre-selected for each particular problem (such as sea conditions, initial conditions, etc.).

Accelerations

$$\dot{u} = \frac{1}{m-X_u} \left\{ X_{(hull)} + X_{(props)} + X_{(rudders)} + X_{(wind)} + X_{(waves)} + X_{(beach)} + mvr \right\} \quad (A-1)$$

$$\dot{v} = \frac{1}{m-Y_v} \left\{ Y_1 uv + (Y_2 - m)ur + Y_{(props)} + Y_{(rudders)} + Y_{(wind)} + Y_{(waves)} \right\} \quad (A-2)$$

$$\ddot{z} = \frac{1}{m+2lA'_{33}} \left\{ -2lA'_{33}u\dot{\theta} - 2lN'_{zz}(\dot{z}+u\theta) - 2\rho g l Bz + Z_{(waves)} \right\} \quad (A-3)$$

$$\ddot{\phi} = \frac{1}{I_{xx} - K_p} \left\{ K_p \dot{\phi} - W |GM| \phi + K_{(waves)} \right\} \quad (A-4)$$

$$\ddot{\theta} = \frac{1}{I_{yy} + \frac{2}{3} \ell^3 A'_{33}} \left\{ \begin{aligned} & \frac{2}{3} \ell A'_{33} (u\dot{z} + u^2 \theta) - \frac{2}{3} \ell^3 N'_{zz} \dot{\theta} - \frac{2}{3} \rho g B \ell^3 \theta \\ & + M_{(waves)} \end{aligned} \right\} \quad (A-5)$$

$$\dot{r} = \frac{1}{I_{zz} - N_r} \left\{ \begin{aligned} & N_1 u r + N_2 r |r| + N_3 u v + N_{(props)} + N_{(rudders)} \\ & + N_{(control)} + N_{(wind)} + N_{(waves)} \end{aligned} \right\} \quad (A-6)$$

Velocities and Displacements

Velocities and displacements are determined by integration, leading to typical results such as

$$u = \int_0^t \dot{u} dt, \text{ etc.} \quad (A-7)$$

and

$$\psi = \int_0^\psi r dt + \psi(0) \quad (A-8)$$

Kinematics

In addition to the above equations, kinematic relations providing craft position in space with respect to the inertial reference frame are necessary. These relations are obtained from Equations (52) and (53) and are expressed as

$$x_0 = \int_0^t u dt \cdot \cos \psi - \int_0^t v dt \cdot \sin \psi \quad (A-9)$$

$$y_0 = \int_0^t v dt \cdot \cos \psi + \int_0^t u dt \cdot \sin \psi \quad (A-10)$$

for the condition when proceeding toward shore (heavy configuration), and

$$x_o = \int_0^t v dt \cdot \sin \psi - \int_0^t u dt \cdot \cos \psi \quad (\text{A-11})$$

$$y_o = - \int_0^t v dt \cdot \cos \psi - \int_0^t u dt \cdot \sin \psi \quad (\text{A-12})$$

when going seaward from the beach (light configuration).

Hull Forces

$X_{(\text{hull})}$ is given by

$$X_{(\text{hull})} = X_1 u |v| + X_2 vr \quad (\text{A-13})$$

for the heavy configuration, and by

$$X_{(\text{hull})} = X_2 vr + X_3 v^2 \quad (\text{A-14})$$

for the light configuration. All the hull forces for other modes of motion are expressed in the acceleration expressions in Equations (A-1) - (A-6).

Propeller Forces

$X_{(\text{props})}$ is represented by Equations (88) and (90) for the heavy configuration, and by Equations (91) and (92) for the light configuration. (A-15)

The rotational speeds of the port and starboard propellers are represented by n_p and n_s (in rps) and the operating propeller speed used in the propeller force equations is defined as

$$n_o = \frac{1}{2} (n_p + n_s) \quad (\text{A-16})$$

$Y_{(\text{props})}$ is represented by Equation (84) for the heavy configuration, and by Equation (86) for the light configuration. (A-17)

$N_{(\text{props})}$ is given by Equation (85) for the heavy configuration, and by Equation (87) for the light configuration. (A-18)

Rudder Forces

$X_{(rudders)}$ is given by

$$X_{(rudders)} = - 2.8u^2\delta^2 \quad (A-19)$$

$Y_{(rudders)}$ is given by

$$Y_{(rudders)} = 2.71 u^3\delta \quad (\text{heavy}) \quad (A-20)$$

$$Y_{(rudders)} = 0.47 u^2\delta \quad (\text{light}) \quad (A-21)$$

$N_{(rudders)}$ is given by

$$N_{(rudders)} = - 56.69 u^3\delta \quad (\text{heavy}) \quad (A-22)$$

$$N_{(rudders)} = 12.28 u^3\delta \quad (\text{light}) \quad (A-23)$$

where δ is expressed in terms of radians.

Control Moment

The yawing control moment due to differential propeller thrust is given by Equation (110), using the propeller thrust representation for either the heavy or light configuration given in Equations (104) and (105), as the particular case requires. (A-24)

Wind Forces

$X_{(wind)}$ is given by Equation (164); $Y_{(wind)}$ is given by Equation (165); and $N_{(wind)}$ is given by Equation (166). These terms are expressed in terms of parameters defined in Equations (158) - (161). (A-25)

Beach Forces

$X_{(beach)}$ is given by Equation (167) and the associated discussion related to that equation in the text of the report. (A-26)

Wave Forces

X (waves) is represented by Equation (127), followed by a transition region (involving "blending" of force representations, to be discussed when considering wave effects) and then the representation given by Equation (142). This is followed by Equation (152) when the craft is in the run-up region following breaking (a discussion of the particular region and the timing operations to apply to the run-up are given in this Appendix). Another part of the longitudinal wave force is given by Equation (134), which is added to the above when the craft is in the region of oscillatory-type waves, in transition, and when in the solitary wave region, where all of these expressions are valid for the heavy configuration approaching the shoreline. For the light configuration the wave force is represented by Equation (153) in the run-up region, followed by Equation (142) with the sign of u changed and then through transition into Equation (127) with the sign of u changed. To this is added Equation (135) in the region of solitary waves through transition into the oscillatory-type wave region. (A-27)

Y (waves) is given by Equation (128), followed by a transition into the expression in Equation (148). This is then followed by Equation (154) in the run-up region, where all of those expressions are valid for the heavy configuration. For the light configuration the lateral wave force is given by Equation (154), followed by Equation (147), and then Equation (128), where the sign of u is changed throughout these expressions to reflect the altered orientation of the craft. (A-28)

Z (waves) is given by the sum of Equations (124) and (125), followed by a transition to Equations (144) and (146). Then following breaking by Equation (156), with the definitions in Equations (170) - (172), where the results are for the heavy configuration. For the light configuration the vertical wave force is given by Equation (155), followed by the sum of Equations (144) and (146), and

then by the sum of Equations (124) and (125), where the signs of the terms in these last equations (Equations (144), (146), (124) and (125)) are changed. In addition the sign of u is also changed throughout these expressions.

(A-29)

$K_{(waves)}$ for the heavy configuration is given by Equation (131), followed by Equation (150) after transition into the solitary wave region. After breaking no other roll moment is assumed to act on the craft due to any wave action. For the light configuration $K_{(waves)}$ is represented in the solitary wave region by Equation (150), and then by Equation (131), where the sign of u is changed in these expressions for this case.

(A-30)

$M_{(waves)}$ for the heavy configuration is given by Equation (126), followed by transition into the sum of Equations (145) and (147). This is then followed by Equation (157) in the run-up region. For the light configuration $M_{(waves)}$ is given by Equation (157), followed by the sum of Equations (145) and (147) in the solitary wave region, and then by Equation (126) after the transition zone. The sign of u is changed in all the expressions above for the light configuration.

(A-31)

$N_{(waves)}$ for the heavy configuration is given by Equation (130), followed by transition into Equation (149), and then following breaking by Equation (155) in the run-up region. For the light configuration $N_{(waves)}$ is given by Equation (155), followed by Equations (149) and then Equation (130) after transition. The signs of the terms in Equations (149) and (130) are changed, and also the sign of u wherever it appears in these equations for the light configuration.

(A-32)

A flow diagram for solution of the equations developed in this study is given in Figure A-1. All of the constituent elements presented in this Appendix are shown there, together with reference to particular equations, descriptive paragraphs, or other explanatory sources in the Appendix. This will relate all of the terms and operations required in carrying out a computer simulation using these equations.

When treating the waves, and from them the wave forces, a specific sequence of operations is required to represent the wave form and forces. An illustration of the procedures, with reference to specific equations in the body of the report, is given in Figure A-2 for the oscillatory-type waves and in Figure A-3 for solitary waves. Since the wave forces and moments contain the same functional expressions as the wave form expressions, their computation readily follows after the waves are determined.

The separate regions where different types of waves are present are defined by the following:

$$\text{Oscillatory region, } h > .04 \lambda_0 + 1.35 H_0 \quad (\text{A-33})$$

$$\text{Solitary region, } h < .04 \lambda_0 + 1.35 H_0 \quad (\text{A-34})$$

$$\text{Run-up region, when } \frac{H}{h} \geq \frac{5}{7} \quad (\text{A-35})$$

where h is local depth, H_0 is the offshore significant wave height, λ_0 is the representative offshore wavelength (taken from period of maximum spectral energy), and H is the solitary wave height (computed continuously, although not used beyond breaking). Methods of determining the breaking location as well as the timing sequence for initiating run-up functions are discussed in a later section of this Appendix.

The method of selecting the appropriate wave forces for inclusion in the flow diagram of Figure A-1 is illustrated in Figure A-4. Within that diagram the operation of "sum all i's" means the summation of all the separate contributions of the elemental waves that make up the offshore spectrum ($i = 1 \rightarrow 8$ chosen for the present case), and similarly for the wave forces and moments from each of the component terms. The "blend" operation in that figure refers to the transition treatment for the various wave forces as well as the wave form itself, when combining oscillatory and solitary wave terms in the transition region. This region is assumed to be of length L , the boat length, and extends $\pm \frac{L}{2}$ in either side of the transition location given by Equation (25) in the text (or by the equality of the relations in Equations (A-33) and (A-34)). For the case of the wave motion as an example, when approaching the beach from seaward, the blended wave elevation is represented by

$$\eta = \left(\frac{L-\bar{x}}{L} \right) \eta_{osc.} + \frac{\bar{x}}{L} \eta_{sol.} \quad (A-36)$$

where $\eta_{osc.}$ can be held constant at the last calculated value before entering the transition region. The quantity \bar{x} is defined as

$$\bar{x} = x_o - \left(x_t - \frac{L}{2} \right) \quad (A-37)$$

which is the distance penetrated into the transition zone, where x_t is the distance along the x_o -axis from the origin to the transition location (Equation (25)). When coming off the beach and proceeding seaward, the last solitary wave values are held constant in the computation of Equation (A-36), and the value of \bar{x} is given by

$$\bar{x} = \left(x_t + \frac{L}{2} \right) - x_o \quad (A-38)$$

The location where solitary waves break and run-up onto the beach can be calculated directly from the selected offshore wave spectrum characteristics and beach slope. It has been previously shown, See Equation (25) that these same parameters also determine the transition point at which the oscillatory waves become solitary waves. Denoting the depth at which transition occurs as h_t , and assuming the initial solitary wave height at transition to be equal to the significant wave height of the offshore wave spectrum, H_o , the height of a solitary wave as it progresses toward the beach is governed by Equation (27) with $h_1 = h_t$ and $H_1 = H_o$ until a wave height to local depth ratio of .714 ($= \frac{5}{7}$) is obtained (Equation (26)). Combining these equations and solving for the depth at which breaking occurs gives

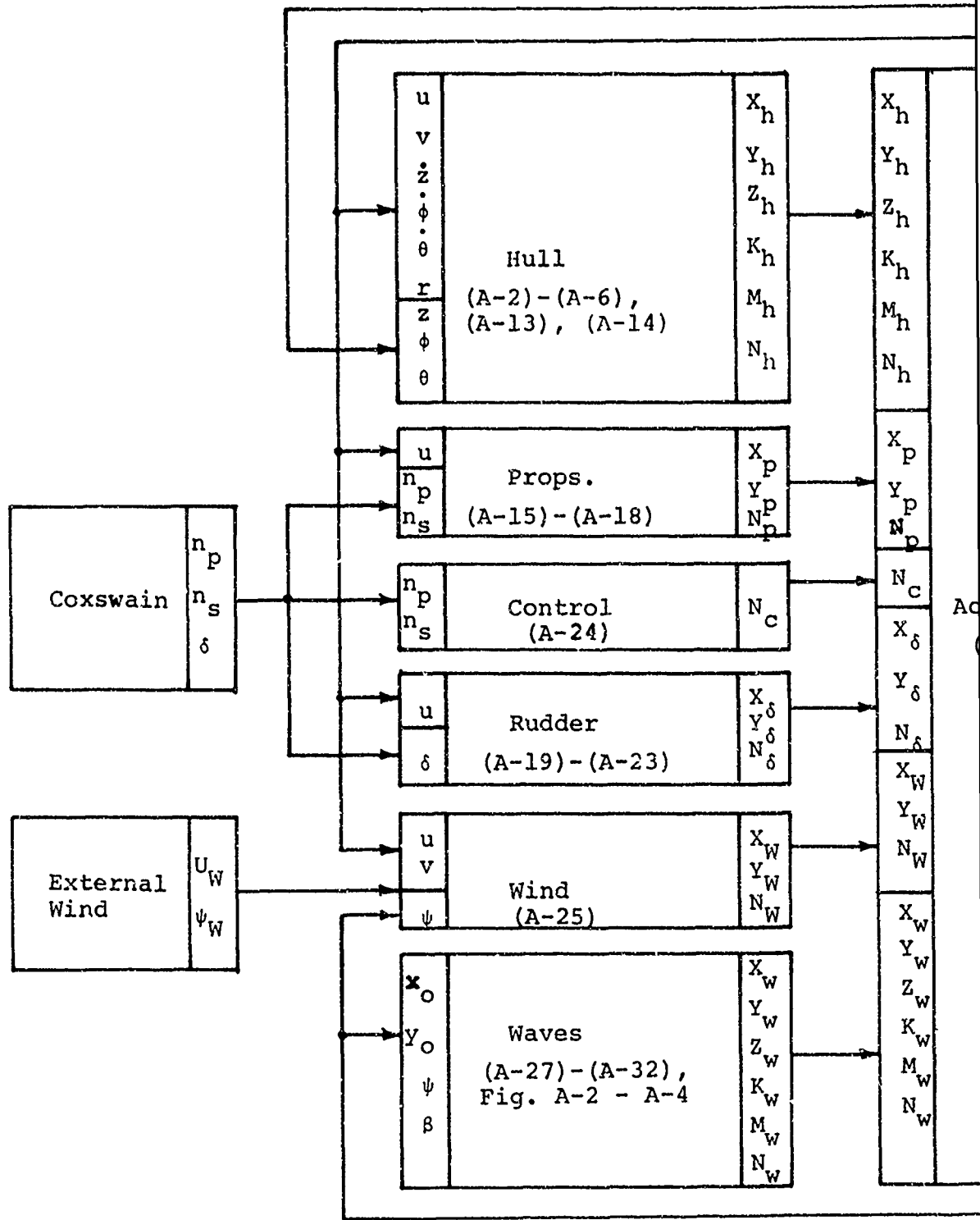
$$h_b = \left[h_t \left(\frac{H_o}{.714} \right)^4 \right]^{1/5} \quad (A-39)$$

which, in turn, knowing the beach slope, determines the distance X_{ob} . It is important to realize that breaking of a solitary

wave may not occur at the time the landing craft reaches the breaking point and, in fact, the coxswain should attempt to avoid this situation by adjusting the boat speed so that the boat follows behind a solitary wave and its resulting run-up onto the beach.

The run-up is synchronized in time with the arrival of a solitary wave at the breaking point, X_{ob} , by simply replacing

time, t , in all run-up functions with $t + \frac{T}{2}$. This is due to the offset of $\frac{T}{2}$ seconds introduced in Equation (168) to achieve the proper time characteristics of the hyperbolic functions.



A:

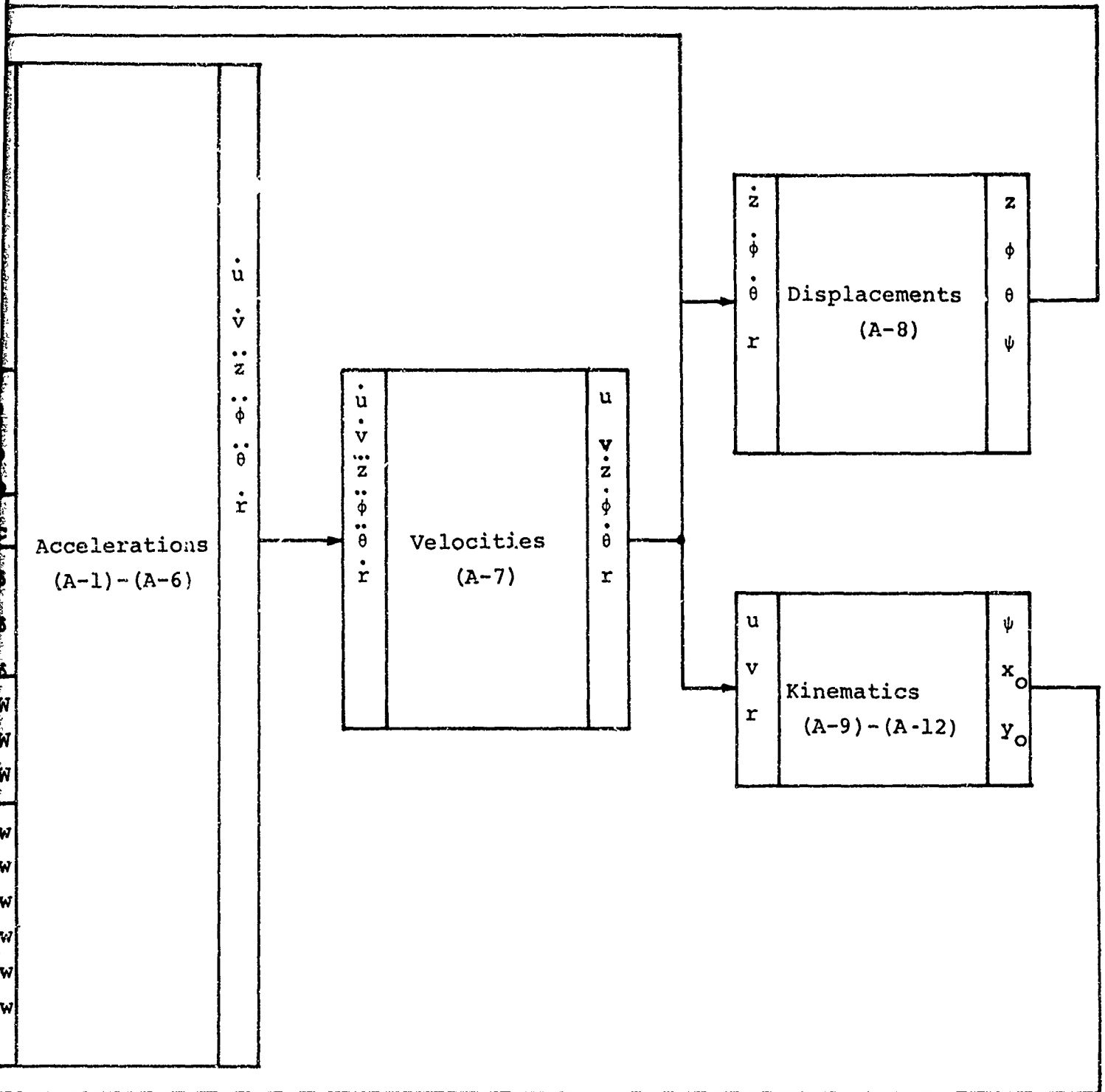


Figure A-1. Flow diagram for solution of equations of motion

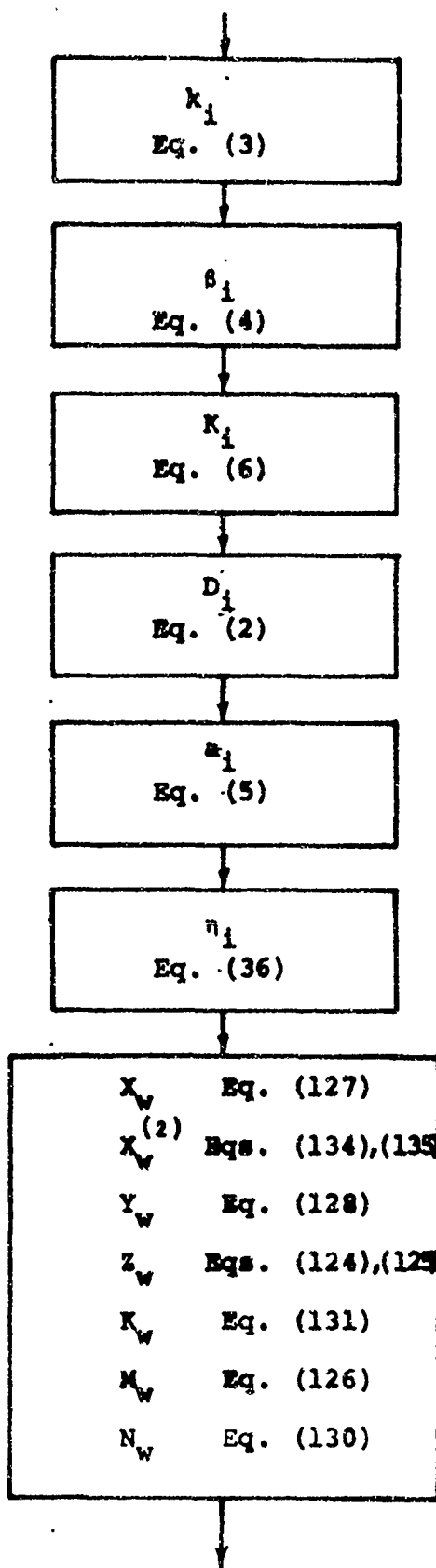


Figure A-2. Flow chart for determining oscillatory wave form and forces

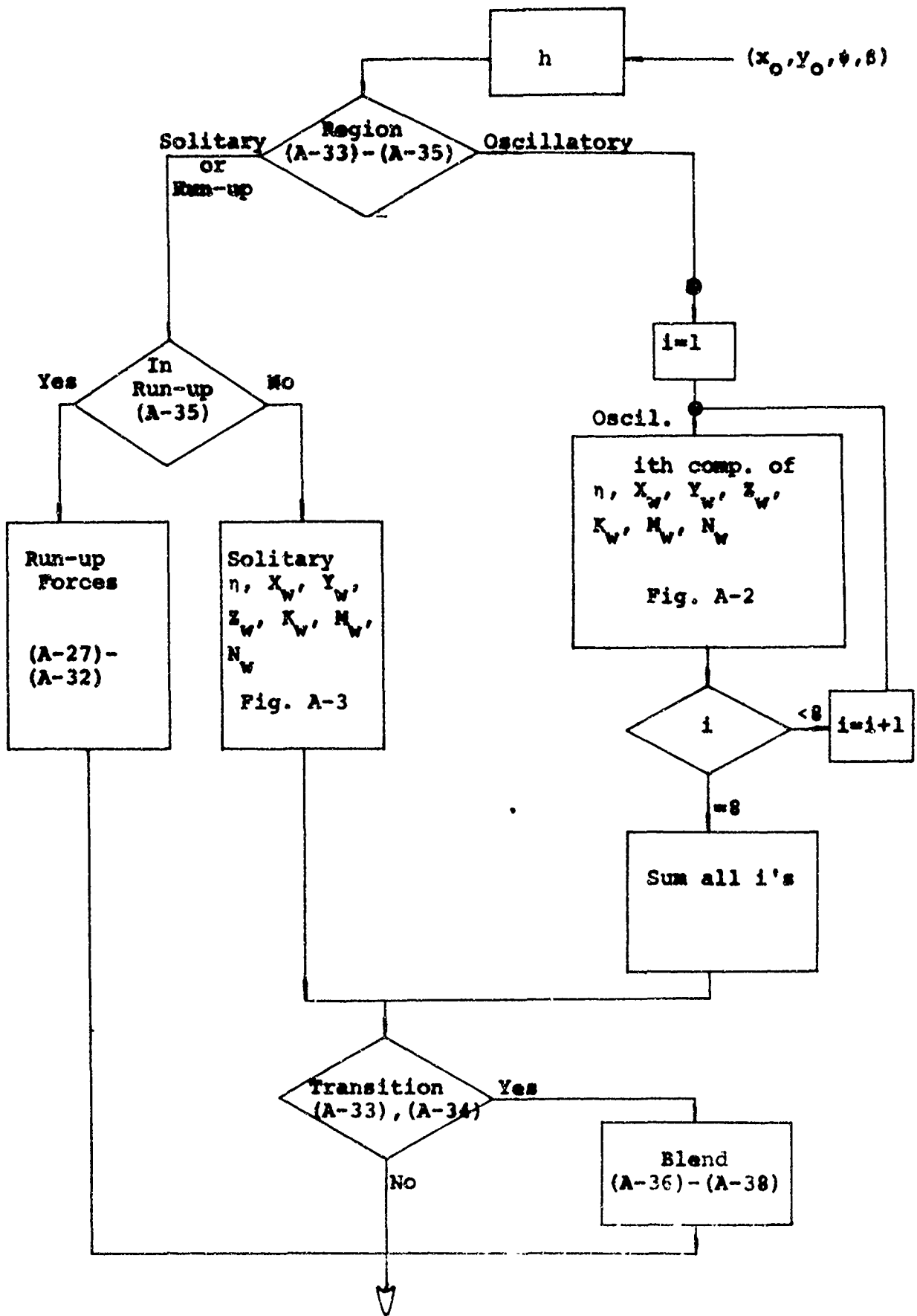


Figure A-4. Procedure for selecting wave forces
79/80

UNCLASSIFIED

Security Classification

DOCUMENT CONTROL DATA - R & D

Security classification of title, body of abstract and indexing annotation must be entered when the overall report is classified

1 ORIGINATING ACTIVITY (Corporate author) OCEANICS, Inc. Technical Industrial Park Plainview, New York 11803		2a. REPORT SECURITY CLASSIFICATION Unclassified	
		2b. GROUP	
3 REPORT TITLE A MATHEMATICAL MODEL FOR ASSAULT BOAT MOTION IN WAVES			
4 DESCRIPTIVE NOTES (Type of report and inclusive dates) Final Report, March 1968-June 1969			
5 AUTHOR(S) (First name, middle initial, last name) Paul Kaplan, Lawrence W. Ward and Theodore P. Sargent			
6 REPORT DATE June 1969		7a. TOTAL NO OF PAGES 83	7b. NO OF REFS 26
8a. CONTRACT OR GRANT NO N61339-68-C-0152		9a. ORIGINATOR'S REPORT NUMBER(S) Tech. Rpt. No. 69-65	
b. PROJECT NO 8186		9b. OTHER REPORT NO(S) (Any other numbers that may be assigned this report)	
c.			
d.			
10 DISTRIBUTION STATEMENT This document has been approved for public release and sale; its distribution is unlimited.			
11 SUPPLEMENTARY NOTES		12 SPONSORING MILITARY ACTIVITY Naval Training Device Center Orlando, Florida 32813	
13 ABSTRACT A six degree of freedom mathematical model of an assault boat landing on and retracting off a sloping beach through surf is developed based on both theoretical and experimental results. Included are the effects of wave refraction, winds, shoaling breaking and wave run-up on the beach. Control forces and moments resulting from the coxswain ability to alter the throttles and rudders are also included. This report is to serve as a basis for the development of a real time assault boat simulator for the training of coxswains.			

DD FORM 1473 (PAGE 1)
NOV 65

DA FORM 1473 (PAGE 1)
NOV 65

UNCLASSIFIED

Security Classification

UNCLASSIFIED

Security Classification

14 KEY WORDS	LINK A		LINK B		LINK C	
	ROLE	WT	ROLE	WT	ROLE	WT
WAVES, SHALLOW WATER						
MATHEMATICAL MODEL						
COMPUTER SIMULATION						
LANDING CRAFT LCM (6)						
SEA SIMULATION						
SHIP MOTION						

UNCLASSIFIED

Security Classification